Herpetological Monographs, 18, 2004, 90–126

PHYLOGENY, ECOMORPHOLOGICAL EVOLUTION, AND HISTORICAL BIOGEOGRAPHY OF THE *ANOLIS CRISTATELLUS* SERIES

MATTHEW C. BRANDLEY[1,3,4] AND KEVIN DE QUEIROZ[2]

[1]*Sam Noble Oklahoma Museum of Natural History and Department of Zoology, The University of Oklahoma, Norman, OK 73072, USA*
[2]*Department of Zoology, National Museum of Natural History, Smithsonian Institution, Washington, DC 20560, USA*

ABSTRACT: To determine the evolutionary relationships within the *Anolis cristatellus* series, we employed phylogenetic analyses of previously published karyotype and allozyme data as well as newly collected morphological data and mitochondrial DNA sequences (fragments of the 12S RNA and cytochrome *b* genes). The relationships inferred from continuous maximum likelihood reanalyses of allozyme data were largely poorly supported. A similar analysis of the morphological data gave strong to moderate support for sister relationships of the two included distichoid species, the two trunk-crown species, the grass-bush species *A. poncensis* and *A. pulchellus*, and a clade of trunk-ground and grass-bush species. The results of maximum likelihood and Bayesian analyses of the 12S, cyt *b*, and combined mtDNA data sets were largely congruent, but nonetheless exhibit some differences both with one another and with those based on the morphological data. We therefore took advantage of the additive properties of likelihoods to compare alternative phylogenetic trees and determined that the tree inferred from the combined 12S and cyt *b* data is also the best estimate of the phylogeny for the morphological and mtDNA data sets considered together. We also performed mixed-model Bayesian analyses of the combined morphology and mtDNA data; the resultant tree was topologically identical to the combined mtDNA tree with generally high nodal support. This phylogenetic hypothesis has a basal dichotomy between the Hispañolan distichoids and the *bimaculatus* series, on the one hand, and the *cristatellus* series inhabiting the Puerto Rican Island Bank, its satellite islands, the Bahamas, and St. Croix, on the other. The trunk-crown species form a clade, while the trunk-ground and grass-bush species do not as *A. gundlachi*, a trunk-ground species, is nested within a clade of grass-bush species. The patterns of relationships among the trunk-ground and grass-bush species suggest that one of these ecomorphs may have been ancestral to the other and that one or both evolved convergently. In the context of our preferred phylogeny and divergence dates estimated by NPRS analyses, we propose several biogeographical hypotheses that explain the current distribution of the *cristatellus* series. The presence of endemic species on the islands of the Bahamas, Desecheo, Mona, Monita, and St. Croix are likely due to over-water dispersal. Vicariance resulting from Pliocene or Pleistocene changes in sea levels likely explains the occurrence of *A. cristatellus* (including *A. ernestwilliamsi*), *A. pulchellus*, and *A. stratulus* on different islands of the Puerto Rican Bank.

Key words: Bayesian; Caribbean Biogeography; Ecomorphology; Frequency coding; Maximum likelihood; Mixed-model; Puerto Rico Bank; Taxonomy.

ANOLIS LIZARDS of the Greater Antilles are of particular interest to evolutionary biologists because they represent a striking case study of convergent evolution and adaptive radiation (Beuttell and Losos, 1999; Losos 1990, 1992, 1994; Losos and de Queiroz, 1997; Williams 1972, 1983). Each of the islands of Cuba, Jamaica, Hispañola, and Puerto Rico is inhabited largely by endemic species of anoles, yet the anole communities of the different islands are remarkably similar in terms of the ecomorphological adaptations of their component species. These communities consist of species with different body plans, called ecomorphs, each of which is morphologically adapted to the structural microhabitat in which it occurs. Ecomorph names correspond to their associated microhabitats: trunk-crown, trunk-ground, grass-bush, crown giant, and twig (Williams, 1983). Higher-level phylogenetic studies based on morphology (Etheridge, 1959; Guyer and Savage, 1986; Poe, 1998; Williams, 1989) and mitochondrial DNA (Jackman et al., 1997, 1999; Losos et al., 1998) have demonstrated that, for the most part, the same set of ecomorphs (or a subset)

[3] CURRENT ADDRESS: Museum of Vertebrate Zoology and Department of Integrative Biology, 3101 Valley Life Sciences Bldg, University of California, Berkeley, CA 94720, USA.
[4] CORRESPONDENCE: e-mail, brandley@berkeley.edu

TABLE I.—Species of the *Anolis cristatellus* series included in this study, with distributions (from Schwartz and Henderson, 1991) and ecomorph designations (from Losos and de Queiroz, 1997).

Species	Locality	Ecomorph class
A. acutus	St. Croix (Virgin Islands)	Unclassified[1]
A. evermanni	Puerto Rico	Trunk-crown
A. stratulus	Puerto Rico and Virgin Islands	Trunk-crown
A. cooki	Puerto Rico	Trunk-ground
A. cristatellus	Puerto Rico and Virgin Islands	Trunk-ground
A. desechensis	Isla Desecheo (Puerto Rico)	Trunk-ground[2]
A. ernestwilliamsi	Carrot Rock (British Virgin Islands)	Trunk-ground[3]
A. gundlachi	Puerto Rico	Trunk-ground
A. monensis	Isla Mona and Monita (Puerto Rico)	Trunk-ground[2]
A. scriptus	Southern Bahamas, Turks and Caicos Islands	Trunk-ground
A. krugi	Puerto Rico	Grass-bush
A. poncensis	Puerto Rico	Grass-bush
A. pulchellus	Puerto Rico and Virgin Islands	Grass-bush

[1] But closest to trunk-crown (Losos and de Queiroz, 1997).
[2] Descendants of trunk-ground ecomorphs, but possess a generalized or trunk-ground morphology (Losos and de Queiroz, 1997).
[3] Ecomorph status not confirmed morphometrically.

has evolved *in situ* on each of the four Greater Antillean Islands.

While studies of higher level *Anolis* phylogenetics continue, several recent studies have addressed the question of the evolutionary relationships within smaller groups of *Anolis*, including the *roquet* series of the Southern Lesser Antilles (Creer et al., 2001), the *bimaculatus* series of the Northern Lesser Antilles, (Schneider et al., 2001), the *grahami* series of Jamaica (Jackman et al., 2002), and the beta section or *Norops* (Nicholson, 2002). In keeping with this trend, we present a phylogenetic study of the *cristatellus* series. For the remainder of the paper, the term "*cristatellus* series" will refer to the taxon that Gorman et al. (1980*a*, 1983) termed the *cristatellus* subseries (excluding the distichoids = the *distichus* subgroup of Williams, 1976). This group also corresponds to the *cristatellus* series of Etheridge (1959) with the addition of *A. acutus*, *A. evermanni*, and *A. stratulus* from his *bimaculatus* series and excluding the cybotoid anoles (= the *cybotes* subseries and species group of Williams, 1976) of Hispañola (see Jackman et al., 1999; Gorman et al., 1980*a*), with the *cristatellus* subseries of Williams (1976) plus *A. acutus*, *A. evermanni*, and *A. stratulus*, with the *cristatellus* series of Savage and Guyer (1989) minus *A. eugenegrahami* (see Williams, 1989), and the distichoids and with the *cristatellus* series of Burnell and Hedges (1990) (Table 1).

The *cristatellus* series consists of approximately 13 currently recognized species that inhabit Puerto Rico and surrounding islands (Virgin Islands including St. Croix, Mona and Monita Islands, and Desecheo Island), although *A. scriptus* inhabits the Bahamas (Schwartz and Henderson, 1991; Fig. 1). The Puerto Rican members of the *cristatellus* series represent three of the five ecomorphs that inhabit the island: trunk-crown (*A. evermanni*, *A. stratulus*), trunk-ground (*A. cooki*, *A. cristatellus*, *A. gundlachi*), and grass-bush (*A. krugi*, *A. poncensis*, *A. pulchellus*) (Williams, 1983); the representatives of the other two ecomorphs, *A. cuvieri* (crown-giant) and *A. occultus* (twig), are relatively distantly related (Jackman et al., 1997, 1999; Gorman et al., 1980*a*; Losos et al., 1998; Guyer and Savage, 1986; Williams, 1989) and represent lineages that either colonized Puerto Rico separately or were already present when the Puerto Rican Bank became isolated from other landmasses.

A series of studies based on allozymes (Gorman et al., 1980*b*, 1983), karyotypes (Gorman et al., 1968, 1983; Gorman and Stamm, 1975), and immunological data (Gorman et al., 1980*a*) dealt explicitly with phylogenetic relationships within the *cristatellus* series. One broad conclusion from these studies is that the basal division in the *cristatellus* series is between a clade of trunk-crown anoles and a clade of grass-bush and trunk-ground anoles. Several osteological features also support the latter clade (Etheridge, 1959; Williams, 1972).

The relationships of the Hispañolan and Bahamian distichoids (the *distichus* subgroup

FIG. 1.—Map of the eastern Greater Antilles. The *cristatellus* series inhabits the islands shown east of Hispañola as well as parts of the Bahamas. Contours indicate ocean depths of 200 and 1000 m.

of Williams [1976], which currently includes *A. altavelensis*, *A. brevirostris*, *A. caudalis*, *A. distichus*, *A. marron*, and *A. websteri* [Burnell and Hedges, 1990], but not *A. eugenegrahami* [Williams, 1989]) to the *cristatellus* series are uncertain. Etheridge (1959) and Williams (1976) placed the distichoids, along with *A. acutus*, *A. evermanni*, and *A. stratulus* in the *bimaculatus* series. Gorman et al. (1980*a*, 1983) placed the distichoids and these other three species in a group exclusive of other anoles (their *acutus* species group). Recent studies have refuted the hypothesized relationship of the distichoids to *A. acutus*, *A. evermanni*, and *A. stratulus*, but have been unable to infer the precise placement of the distichoids with stong stupport. Jackman et al. (1999) weakly placed the distichoids as sister to the *cristatellus* series, whereas Poe (2004) found weak support for their placement as sister to the *bimaculatus* series.

Despite past phylogenetic work, certain relationships within the *cristatellus* series are uncertain, especially those of *A. acutus* and *A. gundlachi*. *Anolis acutus* of St. Croix possesses what may be considered a generalist body plan and does not fit into any recognized ecomorph class (Losos and de Queiroz, 1997). A previous phylogenetic study based on allozymes and karyotypes either placed it sister to the trunk-ground and grass-bush species exclusive of *A. gundlachi*, or was unable to resolve its relationships, depending on the analysis (Gorman et al., 1983). An immunological study placed *A. acutus* closer to *A. cristatellus* (a trunk-ground species) than to *A. stratulus* (a trunk-crown species) (Gorman et al., 1980*a*). *Anolis gundlachi*, a trunk-ground species, shares a derived karyotype with the grass-bush anoles (Gorman et al., 1968, 1983), though analyses based on allozymes have been unable to unambiguously determine its phylogenetic relationships (Gorman et al., 1983). It has also been suggested that *A. gundlachi* represents the sister taxon to a clade composed of the grass-bush and other trunk-ground species (Williams, 1972).

Several studies have attempted to elucidate the pattern of ecomorph evolution on Puerto Rico. Williams (1972), making early use of a phylogeny, proposed a basal divergence between the trunk-crown and the grass-bush + trunk-ground species as well as evolution of the grass-bush ecomorph from the trunk ground ecomorph. Losos (1992) concluded that the ancestor was a generalist and proposed a sequence of ecomorph evolution from

generalist to trunk-ground to (separately) trunk-crown and grass-bush. A subsequent analysis of morphology and habitat use by species in one- and two-species communities led Losos and de Queiroz (1997) to hypothesize that the Puerto Rican species of the *cristatellus* series may have descended not from a generalist but from a trunk-crown ancestor. All of these hypotheses, however, were limited by the phylogenetic information available at those times.

Past biogeographic hypotheses for the *Anolis cristatellus* series are few, and are primarily theories based on limited phylogenetic and geological evidence (Gorman, 1980*a*; Williams, 1969). The geology of the Caribbean is complex, but dramatic improvements in the understanding of the geologic history of the region have been made (Pindell and Barret, 1991; Iturralde-Vinent and MacPhee, 1999; MacPhee et al., 2003) since the last thorough phylogenetic treatment of the *cristatellus* series.

The availability of new data and recent advances in analytical methods may help resolve the phylogenetic relationships within the *cristatellus* series and thus shed light on other aspects of its evolution. In this study, we first reevaluate the phylogeny of the *cristatellus* series, and the placement of the distichoids, synthesizing the information in data sets derived from morphological, mtDNA, allozyme and karyotype data. We then use this phylogeny to evaluate hypotheses about ecomorph evolution on Puerto Rico. Specifically, we attempt to assess which ecomorph, if any, represents the ancestral condition of *cristatellus* series anoles on Puerto Rico as well as the subsequent sequence of ecomorph evolution that gave rise to the three *cristatellus* series ecomorphs that exist today on the island. Finally, we incorporate phylogenetic and recent geological evidence as well as relative molecular divergence estimates to make inferences about the biogeographic history of the group.

Materials and Methods

Taxon and Character Sampling of Multiple Data Sets

In the new data sets collected for this study (morphology and DNA), we sampled all recognized species of the *cristatellus* series (Table 1), including *A. ernestwilliamsi* and *A. desechensis*, two species never before included in a phylogenetic analysis. Two distichoids, *A. brevirostris* and *A. distichus*, representing both of the main superspecies (Williams, 1976) or complexes (Arnold, 1980) within this group, were sampled. *Anolis gingivinus* and *A. wattsi*, members of the *bimaculatus* series, and *A. cybotes* served as outgroups. The *bimaculatus* series is thought to be the sister of the *cristatellus* series and *A. cybotes* is more distantly related (e.g., Gorman et al., 1980*a*; Jackman et al., 1999).

Allozymes.—Gorman et al. (1983) presented two allozyme data sets that differ in numbers of both taxa and characters, both of which were reanalyzed for this study. The two allozyme data sets both lack *A. brevirostris*, *A. desechensis*, *A. distichus*, *A. ernestwilliamsi*, *A. gingivinus*, and *A. wattsi*. The two data sets also included outgroup taxa not represented in our DNA and morphological data sets: *A. cuvieri*, *A. occultus*, and *A. oculatus* in the first data set; and *A. carolinensis*, *A. gadovi*, and *A. grahami* in the second. We included these taxa as outgroups in our reanalyses of the allozyme data.

Morphology and karyology.—Two karyotype, 18 scalation, and 13 osteological characters (hereafter referred to as the "morphological" data set; Appendix I) were scored for 13 ingroup species, 3 outgroup species, *A. brevirostris*, and *A. distichus* (Appendix II). An effort was made to sample widely among sex and age classes as well as across geographic ranges and subspecies. Scalation characters were scored on fluid preserved specimens (N = 9–52 per species, median = 13; Appendix III). Cranial characters were scored from dry osteological specimens (N = 1–23 per species, median = 10; Appendix IV). Axial skeleton characters were scored from radiographs and supplemented with data provided by R. Etheridge that had also been collected from radiographs and used in his 1959 study (N = 5–30 per species, median = 17; Appendix III). Karyotype descriptions from Gorman (1973) and Gorman et al. (1983) served as the basis of two separate characters. Karyotype information was not available for *A. brevirostris*, *A. desechensis*, and *A. ernestwilliamsi*.

Several characters displayed ontogenetic variation, including the development of a tail crest (character 19), location of the pineal foramen (22), development of anteroventral shelves on the basipterygoid processes (23), shape of the parietal roof and crests (25), development of dentary sculpturing (27), and size of the labial blade of the coronoid (29). For these characters, only specimens that were at least 85% of the maximum SVL published in Schwartz and Henderson (1991) were scored. If SVL data were not available for osteological specimens, then classification as an adult was determined by comparing the cranial size to specimens known to be ≥85% maximum SVL. Two characters, the presence of a tail crest (19) and dentary sculpturing (27), are sexually dimorphic and therefore were scored only for males.

Because the inclusion of intraspecifically variable characters has been shown to improve phylogenetic accuracy (Wiens, 1995, 2000, 2001; Wiens and Servedio, 1997), we included several such characters. For scale count characters that were variable on the right and left side of the same specimen, each side was scored separately, then summed and divided by two. Character state frequencies per species were calculated as the number of observations of a particular state divided by the total number of observations of all states for the character.

Mitochondrial DNA.—Genomic DNA was extracted from frozen or ethanol preserved liver or muscle tissue using a chloroform/phenol extraction or Qiagen DNeasy™ kits. When possible, two specimens of each species were included. Localities for voucher specimens are provided in Appendix V. A ~650-bp fragment of the cytochrome *b* (cyt *b*) and a ~335-bp fragment of the 12S rRNA genes were amplified using PCR following the protocol of Wilgenbusch and de Queiroz (2001). Two overlapping ~400-bp fragments of cyt *b* were amplified using the primers: L14841: 5′-AAAAAGCTT-CCATCCAACATCTCAGCATGATGAAA-3′, H15149: 5′-AAACTGCAGCCCCTCAGA-ATGATATTTGTCCTCA-3′ and L15066: 5′-AATAAGCTTTTAAAGAAACATGAAAY-ATTGGAGTA-3′, H15496: 5′-AAACTG-CAGGGAATAAAGTTATCTGGGTCTC-3′ (Kocher et al., 1989). For some samples, the entire ~650-bp fragment was amplified using only L14841 and H15496. The 12S fragment was amplified using the primers: 5′-AAACTGGGGATTAGATACCCCACTAT-3′ and 5′-GAGGGTGACGGGCGGTGTGT-3′ (Reeder, 1995). The PCR products were purified using a Promega Wizard™ PCR kit, dye labeled using an ABI Big Dye Terminator™ cycle sequencing kit, and sequenced on an ABI 373™ or 377™ automated sequencer. Sequences were deposited in GenBank (AY534648-534680, AY662309-AY662324).

Cyt *b* sequence alignments were not problematic because of the apparent lack of insertions/deletions and were performed by eye. Because insertions and deletions were present in the 12S rRNA sequences, they were aligned with reference to published secondary structure maps (Hickson et al., 1996; Kjer, 1995; Titus and Frost, 1996). Ambiguous nucleotide positions were determined by creating multiple alignments using Clustal X (Thompson et al., 1997), with gap costs of 5, 10, and 15 (Wiens and Reeder, 1997). Homologous stem regions were forced to align, and gaps were constrained to loops. Nucleotides that changed position with variable gap costs were considered ambiguously aligned and were not used in the phylogenetic analyses. Alignments can be obtained from the first author.

Phylogenetic Analyses

The primary phylogenetic analyses of the allozyme, morphological, and mtDNA data were conducted using maximum likelihood (ML). Most implementations of the ML criterion model the probability of character change as a function of branch length and are thus better able to deal with the phenomenon of long branch attraction, a systematic bias resulting in the tendency of long branches to group together regardless of common descent (Felsenstein, 1978; Hendy and Penny, 1989; Huelsenbeck, 1997). ML also has the ability to accommodate the heterogeneous nature of DNA sequence evolution and has been shown to outperform other phylogenetic methods when diverse conditions are simulated (Huelsenbeck, 1995; Yang, 1996).

Allozymes.—The allozyme data were analyzed using the same continuous maximum likelihood procedures used with the morphological data (see below). Two changes

were made to the data prior to analysis. Because CONTML cannot incorporate missing data, the *Est-1* locus was removed from the first data set. Secondly, if more than one population sample was available for a species, then samples were pooled and mean allelic frequencies per locus were used.

Morphology.—A variety of methods for analyzing polymorphic data have been proposed (reviewed by Wiens, 1999, 2000), but those that best incorporate the quantitative nature of these characters, including continuous maximum likelihood and frequency parsimony methods, tend to outperform other methods (Wiens, 1999, 2000; Wiens and Servedio, 1998). Among other favorable traits, these methods minimize the influence of character states occurring at low frequencies and therefore the influence of sampling errors (Swofford and Berlocher, 1987; Wiens, 2000). Primary phylogenetic analyses were performed using continuous maximum likelihood. Continuous maximum likelihood methods employ restricted maximum likelihood (REML) analyses of quantitative data using a Brownian motion model of evolution (Felsenstein, 1973, 1981, 1985, 1988, 2002). The Brownian motion model assumes that all characters evolve independently and at the same rate. Felsenstein (1988, 2002) suggested transforming the characters so that they possess these two characteristics by removing the covariances and standardizing variances of the characters. Otherwise, the Brownian motion model is violated. The CONTML package of PHYLIP uses a square root transformation of the data, which is expected to result in roughly similar variances of the characters. Although we did not remove covariances, ML methods are robust to model violations under many conditions (Huelsenbeck, 1995), and continuous maximum likelihood has been shown to perform well for both real and simulated data without removing covariances (Wiens, 1998; Wiens and Servedio, 1998).

The states of the morphological characters were treated as frequencies (number of occurrences of a particular state divided by total number of occurrences of all states of the same character within a species). Continuous ML analyses of the data were performed using the CONTML program of PHYLIP (version 3.6a2.1; Felsenstein, 1993). Analyses were conducted using the "global rearrangement" (G) and "jumble" (J, 100 replicates) options. Because CONTML cannot incorporate missing data, several characters were removed from the data set, including the postfrontal condition (character 24), the relationships of the splenial to the coronoid (31), and karyotypes (32 and 33). To incorporate these characters, additional analyses using the MANOB approximation of frequency parsimony (Swofford and Berlocher, 1987; Berlocher and Swofford, 1997) were performed with both the full data set and with characters 24 and 31–33 removed. Data were formatted as FREQPARS files and imported into PAUP*4.0b10 (Swofford, 2001), which automatically generated the Manhattan distance cost matrices used in this method. A heuristic parsimony search using 100 random stepwise addition replicates was performed with TBR branch swapping. Nonparametric bootstrapping was used to evaluate nodal support for the CONTML and MANOB trees (1000 pseudoreplicates; for each pseudoreplicate: 10 jumble replicates with global rearrangements for the CONTML analysis and 10 random stepwise addition replications with TBR for the MANOB analysis).

Mitochondrial DNA.—12S, cyt *b* and combined mtDNA trees were inferred using ML and Bayesian analyses. For the ML analyses, we used a modification of the successive approximation method described by Swofford et al. (1996) and Wilgenbusch and de Queiroz (2000). Initial maximum parsimony (MP) topologies were constructed using a heuristic search with 100 random stepwise addition replicates and TBR branch swapping. If the MP analyses yielded more than one most parsimonious tree, the likelihood scores for the GTR+I+Γ model were calculated for each tree. Using the MP tree (or the MP tree with the best likelihood score) as a starting tree, we used the likelihood ratio test (LRT), implemented by MrModeltest 1.1 (Nylander, 2002; a variant of Posada and Crandall's [1998] Modeltest), to select a model of sequence evolution for use in a subsequent ML tree search. The model parameters and values, including estimated base frequencies, substitution rates, proportion of invariable sites, and gamma shape parameter, were chosen by

MrModeltest and then used in a subsequent ML heuristic search (20 replicates of random stepwise addition, TBR branch swapping). The resultant ML tree was again analyzed using MrModeltest, and another search using the new model parameters and values was initiated in PAUP*. This process was repeated until the same likelihood score and tree were estimated in successive iterations.

Bayesian phylogenetic methods generate estimates of model parameter values, topologies, and branch lengths by periodically sampling this parameter space using Markov Chain Monte Carlo methods (MCMC; Hastings, 1970; Metropolis et al., 1953). Because Bayesian analyses use the likelihood function and the same models of evolution commonly used with ML, Bayesian analyses using uniform prior probabilities are expected to yield similar results as ML (Larget and Simon, 1999). Bayesian analyses of the 12S, cyt *b*, and combined mtDNA were conducted using MrBayes 3.0b4-5 (Huelsenbeck and Ronquist, 2001) using the same models used in the ML analyses. To decrease the chance of converging on a local optimum, four independent analyses based on different, random starting trees were performed for each of the data sets. All four analyses consisted of 10^7 generations and four Markov chains using default heating values. The model was identical to those of the ML analyses with all parameter values estimated and the Markov chains were sampled every 1000 generations. The first 10^6 generations were removed as "burn-in" and stationarity was verified by both plotting the –ln *L* per generation (i.e., "burn-in" plots) and using the program Converge 0.1 (Warren, et al. 2003), which tracks the cumulative posterior probabilities of individual clades. Provided that the four analyses reached stationarity at a similar likelihood score and that the topologies were congruent, the resultant trees were combined using a majority rule consensus tree in PAUP*.

Nodal support for the mtDNA data was assessed in two ways—likelihood non-parametric bootstrapping and Bayesian "posterior probabilities" (this term is used loosely because the values in question are based on uniform prior "probabilities," reflecting a lack of prior information, and thus on the controversial subjective interpretation of probability). The bootstrap analyses used the same model parameters and values estimated from the final round of successive tree searching and consisted of 1000 pseudoreplicates with as-is stepwise addition and TBR branch swapping. Likelihood boostrap proportions are abbreviated "*LBP*" and parsimony, "*BP.*" In all analyses for all data sets, bootstrap proportions $\geq$95% are considered highly supported, $\geq$70% moderately supported, and lesser values weakly supported. "Posterior probabilities" $\geq$95% are considered significant under the commonly accepted criterion of α = 5% (Wilcox et al., 2002) and will be abbreviated "*PP*" throughout the text.

Assessing phylogenetic signal in the highly variable morphological characters and allozyme data sets.—One criticism of using polymorphic or meristic characters in phylogenetic analysis is that they do not contain useful phylogenetic information (Pimentel and Riggins, 1987; Stevens, 1991; reviewed by Wiens, 2001). The g_1 index (Hillis and Huelsenbeck, 1992) and PTP test (Archie, 1990; Faith and Cranston, 1991) were used to assess the presence of phylogenetic signal in the highly variable, polymorphic morphological characters (characters 2–7, 9, 11–13, 17, 26, 30, 31) and in both allozyme data sets. For the g_1 indices, exact *P* values were obtained through the analysis of 100 randomized data sets. Character states were shuffled among taxa within each character using MacClade (Maddison and Maddison, 2000) while the number of character states and their step matricies (if present) were maintained. The g_1 index for each of the 100 randomized data sets (as well as the non-randomized data) was calculated from 10,000 random trees using parsimony. Exact *P* values for the non-randomized data were then calculated from the resultant distribution of the 100 g_1 indices. If the g_1 index of the non-randomized data set fell within the 5% tail of this distribution ($P \leq 0.05$), the data were considered to have non-random phylogenetic signal. PTP tests were conducted with PAUP* using 100 permutation replicates each employing heuristic searches with 10 random addition sequence replicates using maximum parsimony. For the morphological data, g_1 and PTP tests were conducted for both the entire data set and the ingroup taxa only. In addition, parsimony bootstrap analyses (not shown) of these 14 highly vari-

able characters indicated that the only relationship supported with a boostrap proportion ≥70% is that between *A. brevirostris* and *A. distichus*. To determine whether a significant g_1 or PTP value was due solely to this phylogenetic relationship, additional g_1 and PTP tests were performed with *A. brevirostris* removed from the data set. When the g_1 index was determined for a dataset from which taxa were removed, the taxa were removed prior to creating the 100 randomized data sets to eliminate character states unique to them. For the two allozyme data sets, g_1 and PTP tests were only performed after pruning taxa not in common with the morphological and DNA data sets. These tests were conducted to assess whether to include the allozyme data in subsequent combined analyses (see below), and because these taxa would not be used in the combined analyses, their contribution to the overall phylogenetic signal is irrelevant.

Incongruence and phylogenetic hypothesis testing.—We used the SH test (Shimodaira and Hasegawa, 1999) to determine whether each of the data sets strongly support conflicting topologies, and to test whether the data rejected specific phylogenetic hypotheses. SH tests were performed using PAUP* with 10,000 RELL bootstrap replicates.

Combined analyses.—Methods for combining ML analyses performed under models with fundamentally different parameters are still under development. However, because likelihood scores are additive (Edwards, 1972) and comparable across models, we tested different hypotheses by summing the likelihood scores of the different data sets on competing topologies (Wilgenbusch and de Queiroz, 2000). The tree with the best summed likelihood score was considered the best explanation for the combined data (Wilgenbusch and de Queiroz, 2000), under the limitation that only predetermined topologies were compared (as opposed to performing a thorough tree search). The fact that the DNA analyses implement full ML, and the morphological analyses use restricted maximum likelihood (REML), does not invalidate this methodology (J. Felsenstein, personal communication).

We also employed true mixed-model analyses of the combined morphological and DNA data. These analyses permit the use of different, data set specific models in a single analysis. This technique has recently become available in a Bayesian/MCMC framework (MrBayes 3.0; Huelsenbeck and Ronquist, 2001). The mixed-model analysis consisted of a combined mtDNA partition and a morphology partition. The Mkv model (Lewis, 2001) was used for the morphological characters. Because the Mkv model uses discrete character states rather than state frequencies, the morphological data set was recoded using modal values as character states. Because MrBayes crashed when the allozyme data were included, the results of our mixed-model Bayesian analysis are based only on the combined DNA and morphological data.

Ancestral Ecomorph State and Dating Analyses

Ancestral state reconstructions were performed in MacClade using the parsimony criterion with ecomorph status coded as a discrete, unordered states. We ran the analysis three times treating the ecomorph status of *A. acutus* as unknown (coded "?"), as trunk-crown, and as a generalist (4^{th} state). To aid our biogeographic analysis, we used nonparametric rate smoothing (NPRS; Sanderson, 1997) to estimate divergence dates and a topology where branch lengths and branching order indicate time (a "labeled history"; Edwards, 1970). The NPRS method allows for the determination of divergence dates even in the absence of constant rates of molecular evolution (i.e., when data are not "clock-like"). NPRS analyses were conducted with the program r8s 1.50 using the tree and branch lengths from the ML analysis of the combined 12S and cyt *b* data. These dating analyses require at least one fixed calibration point. Recent geologic interpretations hypothesize that the Mona passage, which separates Hispañola from the Puerto Rican Bank, formed 30 MYA or slightly earlier (MacPhee et al., 2003); however, an aerial connection between the two islands may have existed into the mid to late Miocene (16-8 MYA; Iturralde-Vinent and MacPhee, 1999). We assumed, with reservations, that all divergences within the *cristatellus* series occurred after the Hispañola—Puerto Rico split. We thus ran the r8s analysis twice, fixing the age of the basal division in the *cristatellus* series at 8 and 16 MYA. It should be

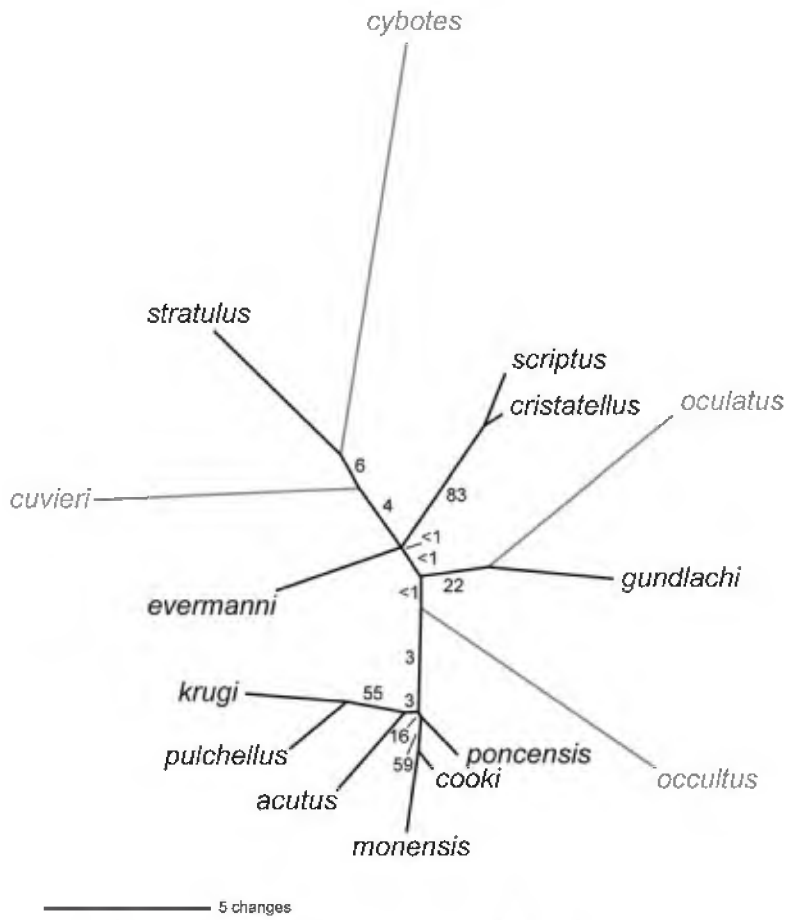

FIG. 2.—Maximum likelihood unrooted phylogram from the CONTML reanalysis of the first allozyme data set of Gorman et al. (1983). Numbers clockwise to the branches are bootstrap proportions. Outgroup taxa are shaded in light grey.

emphasized that the inferred dates for all nodes are therefore dependent on the validity and accuracy of these calibration points. If the aerial contact between Hispañola and Puerto Rico existed earlier or later, or if the diversification of the *cristatellus* series occurred before the breakup of this landmass, the dates inferred by the NPRS analysis may not be accurate. These estimated divergence dates should therefore be considered preliminary until further geologic or paleontological evidence can provide additional calibration points. 95% confidence intervals for each estimated age were constructed using a cutoff of 4 log-likelihood units as suggested in the r8s program documentation.

RESULTS

Allozymes

The CONTML reanalyses of Gorman et al.'s (1983) two allozyme data sets produced trees with low overall bootstrap support. The reanalysis of the first allozyme data set inferred a tree with a ln L = 1016.64. (Note that continuous maximum likelihood can yield both negative and positive log-likelihoods. In the latter case, a larger positive value indicates a better explanation of the data [Felsenstein, 1993]). The tree could not be rooted to maintain ingroup monophyly (Fig. 2), and the sister relationship of *A. scriptus* and *A. cristatellus* is the only node with even moder-

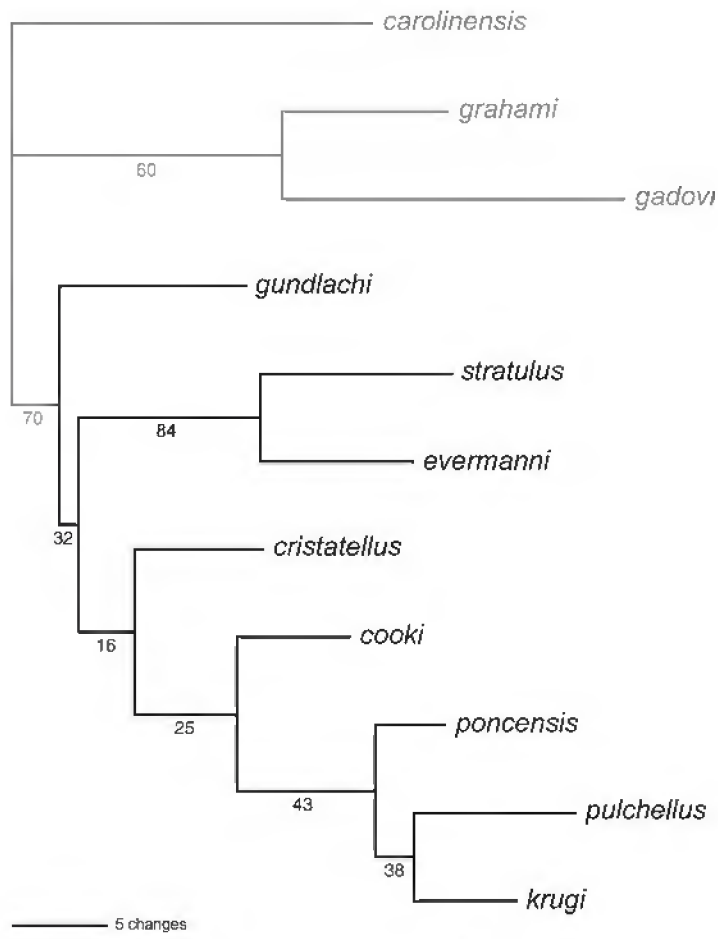

FIG. 3.—Maximum likelihood rooted phylogram from the CONTML reanalysis of the second allozyme data set of Gorman et al. (1983). Numbers below branches are bootstrap proportions. Outgroup taxa are shaded in light grey.

ate support (*LBP* = 83%). The tree from the MANOB reanalysis (not shown) is also largely poorly supported with the *A. pulchellus* and *A. krugi* relationship the only node with even moderate support (*BP* = 75%). The CONTML reanalysis of the second allozyme data set inferred a tree with a ln L = 561.47 (Fig. 3). Monophyly of the *cristatellus* series is moderately supported (*LBP* = 70%), as is the relationship of the two trunk-crown anoles, *A. evermanni* and *A. stratulus* (*LBP* = 84%). The MANOB tree (not shown) had poor support for all nodes with the exception of that uniting *A. evermanni* and *A. stratulus* (*BP* = 83%).

Both g_1 and PTP tests of the pruned first allozyme data set did not reject the null hypothesis of randomized data (P = 0.20, P = 0.13, respectively). Results of these tests for the pruned second alloyzme data set are significant ($P < 0.01$, $P = 0.01$). Because the first allozyme data set does not contain phylogenetic signal that differs significantly from random data, it was not used in the combined data analyses (see below).

Morphology

The results of the g_1 analyses of the highly variable morphological characters are provided in Table 2. Both PTP analyses excluding *A. brevirostris* failed to reject the null hypothesis of random data. These results indicate that at least some of the phylogenetic structure in the most variable morphological characters involves characters uniting *A. brevirostris* and

TABLE 2.—Results of the g_1 skewness and PTP tests for the most highly variable morphological characters.

Data set	Skewness test		PTP test
	g_1 (observed)	P =	P =
All taxa	−0.689	<0.01	<0.01
No *A. brevirostris*	−0.263	0.16	0.26
Ingroup only	−1.004	<0.01	<0.01
Ingroup only, no *A. brevirostris*	−0.408	<0.01	0.09

A. distichus, though the g_1 result is significant (and the PTP suggestive; $P = 0.09$) if both *A. brevirostris* and outgroups are removed. Thus, structure exists in these variable characters, albeit mostly confined to the sister relationship of *A. brevirostris* and *A. distichus*.

The initial CONTML analysis of the morphological data yielded a topology with a $\ln L = 1420.2920$ (Fig. 4). This tree placed the outgroup *A. gingivinus* within the ingroup sister to a clade of the trunk-crown and distichoid anoles, and the outgroup *A. wattsi* sister to the remaining ingroup species. This result is in conflict with conclusions of prior phylogenetic studies based on karyotype (Gorman and Atkins, 1969), allozyme (Gorman and Kim, 1976), immunological (Shochat and Dessauer, 1981), and DNA sequence (Schneider et al., 2001) data, all of which support a close relationship between *A. gingivinus* and *A. wattsi* as members of the *bimaculatus* series. However, these unconventional placements are poorly supported as are all but four other nodes. The MANOB analysis of the full data set yielded a single tree with 110.45 steps (Fig. 5) and a single tree with 95.20 steps for the MANOB analysis excluding the missing data characters (not shown). Although they inferred topologically different trees, no incongruence is even moderately supported and both analyses inferred almost identical support for the three moderate- to well-supported clades (Fig. 5). The fact that the MANOB analyses (both including and excluding the missing data characters) and CONTML analyses did not infer even moderately supported, incongruent nodes demonstrates that the necessary exclusion of some characters from the CONTML analysis was not problematic. The CONTML tree is our preferred morphology-based hypothesis and was used in subsequent analyses based on summed log-likelihoods.

The sister relationship between the distichoid and trunk-crown anoles has low bootstrap support (*LBP* = 59%) but is nonetheless supported by several derived characters. One hundred percent of the specimens of the four species in this clade possess small posterior superciliary scales (character 8) compared with 0% in the sister clade. These taxa also generally lack a median parietal crest (100% of all specimens examined of *A. evermanni* and *A. stratulus*, 90% and 42% in *A. brevirostris* and *A. distichus*; character 25), while the crest is usually present (80–100% of the specimens examined, depending on the species) in adults of the sister clade. The sister relationship between *A. brevirostris* and *A. distichus*, the two distichoid representatives, has high bootstrap support (*LBP* = 100%), and is supported by three derived states found in 100% of the individuals: smooth supradigital scales (character 18), a laterally expanded postfrontal bone (character 24), and a truncated labial process of the coronoid (character 29). *Anolis brevirostris* and *A. distichus* also tend to have low numbers of scales between the second canthal scales (modes of 4 compared with modes ranging from 5–11 in the other species) (character 5). The relationship between the two trunk-crown anoles, *A. evermanni* and *A. stratulus*, is moderately supported (*LBP* = 90%). One hundred percent of the individuals in this clade lack a median parietal crest (character 25), lack a splenial (convergent in *A. poncensis*) (character 28), and possess the intermediate state of the postfrontal bone (character 24). Most individuals of both species have keeled scales of the supraocular disk (character 2), a character not shared with the distichoids, but also present in the remaining *cristatellus* series taxa.

Anolis acutus is placed as the sister taxon to the grass-bush + trunk-ground clade; this relationship is supported by the presence of a derived tail crest (character 19; 100% in *A. acutus* and the trunk-ground anoles, secondarily lost in the grass-bush species). However, the tail crest in the trunk-ground anoles extends much farther above the tail than in *A. acutus*. The presence of keeled ventral scales (character 15) and splenial overlap of the coronoid (character 31), though variable in

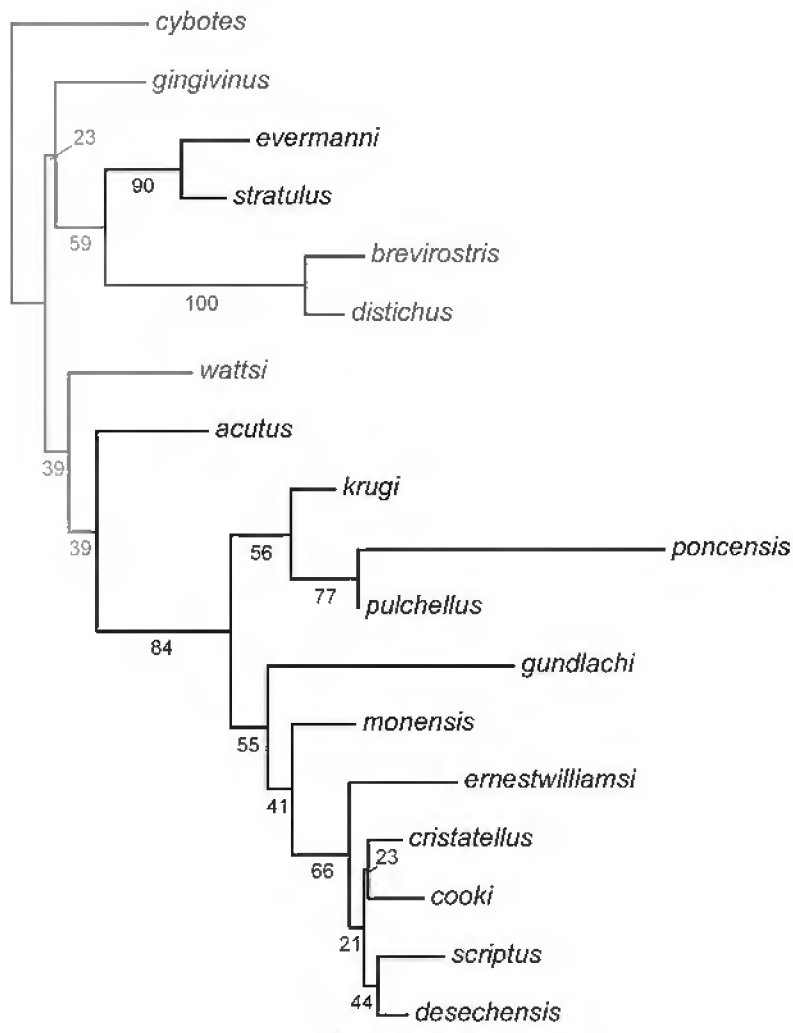

FIG. 4.—Rooted ML phylogram from the CONTML analysis of the morphological data set. Numbers below branches are bootstrap proportions. Outgroup taxa are shaded in light grey and the distichoids in medium grey.

some taxa, also supports the placement of *A. acutus* with the grass-bush and trunk-ground species.

The grass-bush + trunk-ground clade (*LBP* = 84%) is supported by several derived states. One hundred percent of all species examined have 23 (as opposed to 24) presacral vertebrae (character 20), and the vast majority of individuals of each species possess two attached and two free (versus three attached and one free) post-xiphisternal inscriptional ribs (character 21) and keeled (as opposed to smooth) scales of the supraocular disk (character 2). Except for *A. poncensis* and *A. pulchellus* (the two species with the smallest body size), most adults in this clade possess anteroventral shelves on the basipterygoid processes (character 23). In every species except *A. pulchellus* and *A. krugi* a majority of the individuals share the derived condition of the parietal foramen penetrating the parietal rather than the fronto-parietal suture (character 22). Finally, some specimens of all species within the grass-bush + trunk-ground clade possess some form of dentary sculpturing (character 27).

The grass-bush + trunk-ground clade splits into a clade of the grass-bush anoles + *A.*

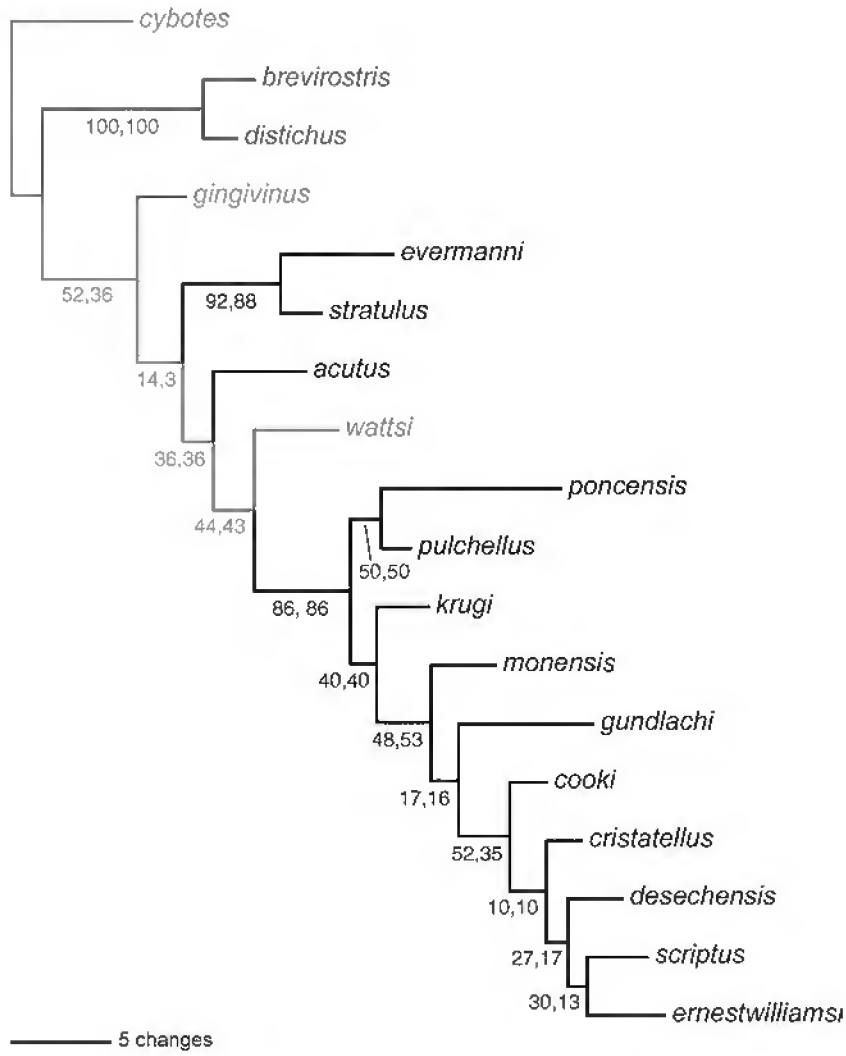

FIG. 5.—Rooted phylogram from the MANOB analysis of the morphological data set including all characters. Numbers below branches are bootstrap proportions. The first value indicates bootstap percentages for the MANOB analysis of the complete character data set. The second value indicates bootstrap proportions for the MANOB analysis of the data set excluding characters 24, 31–33. Outgroup taxa are shaded in light grey and the distichoids in medium grey.

gundlachi and a clade of the remaining trunk-ground species. The former clade is supported by the presence of carinate head scales (character 1) found in 100% of all the individuals except *A. pulchellus* (83%). *Anolis pulchellus* and *A. poncensis* are the only species in this study possessing individuals with reduced toepads (character 16; 100% in *A. poncensis* and 30% in *A. pulchellus*). The sister relationship between *A. poncensis* and *A. pulchellus* is moderately supported (*LBP* = 77%). Among the remaining trunk-ground anoles exclusive of *A. gundlachi*, *A. monensis* is sister to a clade of *A. cooki*, *A. cristatellus*, *A. desechensis*, *A. ernestwilliamsi*, and *A. scriptus* (*LBP* = 66%). Relationships within the latter clade appear to be based primarily on minor frequency differences and are poorly supported. Although part of the clade of trunk ground anoles, *A. monensis* shares several characters with the *A. gundlachi* + grass-bush clade including carinate head scales (character 1; 100%) and *krugi* type dentary sculpturing (character 27; 86%).

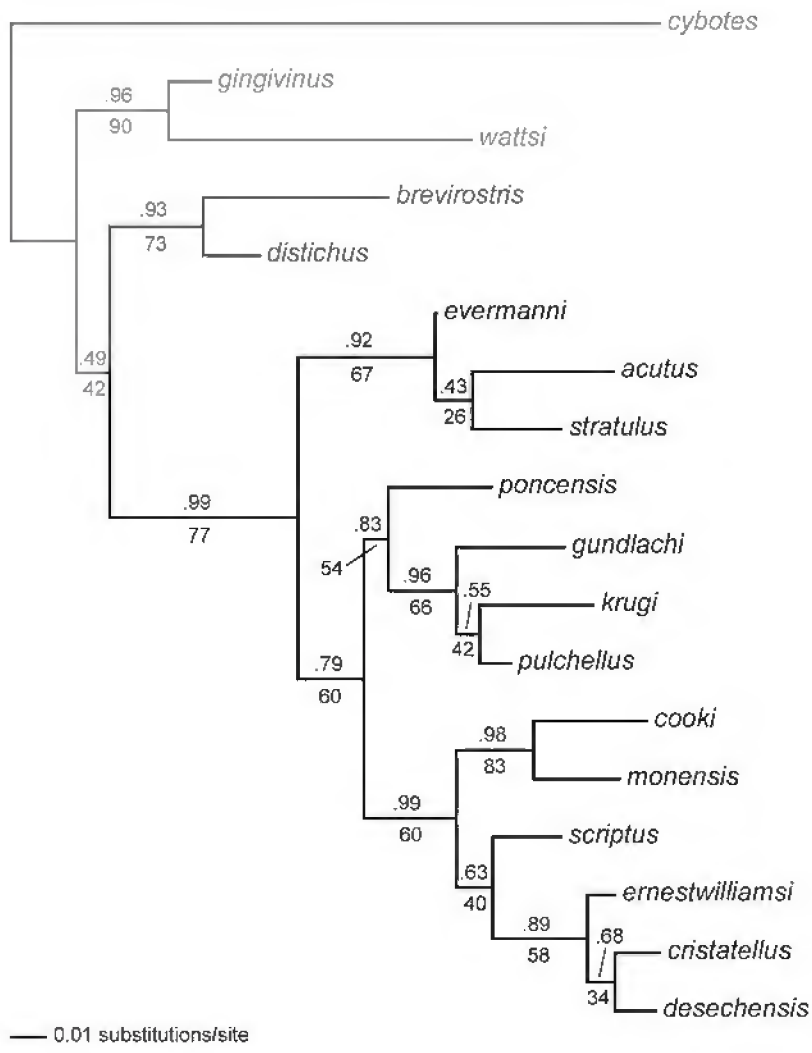

FIG. 6.—Maximum likelihood rooted phylogram for the 12S rRNA mtDNA data set. Numbers above branches are "posterior probabilities," numbers below branches are likelihood bootstrap percentages. Outgroup taxa are shaded in light grey and the distichoids in medium grey.

Mitochondrial DNA

Preliminary phylogenetic analyses demonstrated that each species represented by more than one specimen was monophyletic (not shown). Given this, and the need to make the DNA analyses easily comparable to the morphology and allozymes, these redundant specimens were removed and the phylogenetic analyses were performed again. All further results and discussion will be limited to these single-specimen analyses.

12S.—Thirteen sites were considered ambiguously aligned and were removed from the data set prior to analysis, leaving 320 characters, 93 of which were variable and 51 parsimony-informative. The GTR+I+Γ was the most appropriate model of sequence evolution (according to the LRT) with all iterations of the successive likelihood searches. Parameter estimates for this model are summarized in Table 3. A maximum likelihood analysis using these parameters yielded one

tree with a score ln L = –1414.6175 (Fig. 6). All four Bayesian analyses reached stationarity at a similar mean ln L (≈–1440) and supported the same topology . The posterior probabilities estimated from these analyses are based on 36,000 trees sampled from stationarity and mapped onto the ML tree (Fig. 6).

The distichoids, *A. distichus* and *A. brevirostris*, form a well-supported clade (*LBP* = 73%, *PP* = 0.93) and are weakly placed (*LBP* = 42%, *PP* = 0.49) as the sister to the *cristatellus* series. The *cristatellus* series forms a moderately (*LBP* = 77%) to strongly (*PP* = .99) supported clade of trunk-crown, trunk-ground, and grass-bush species of the Puerto Rican Island Bank and satellite islands. The trunk-crown + *A. acutus* clade (*LBP* = 67%, *PP* = 0.92) is sister to a weakly supported (*LBP* = 60%; *PP* = 0.79) clade of trunk-ground and grass-bush anoles. *Anolis poncensis*, a grass-bush anole, is sister to a poorly (*LBP* = 66%) to well-supported (*PP* = 0.96) clade of *A. krugi* and *A. pulchellus*, also grass-bush anoles, and *A. gundlachi*, a trunk-ground

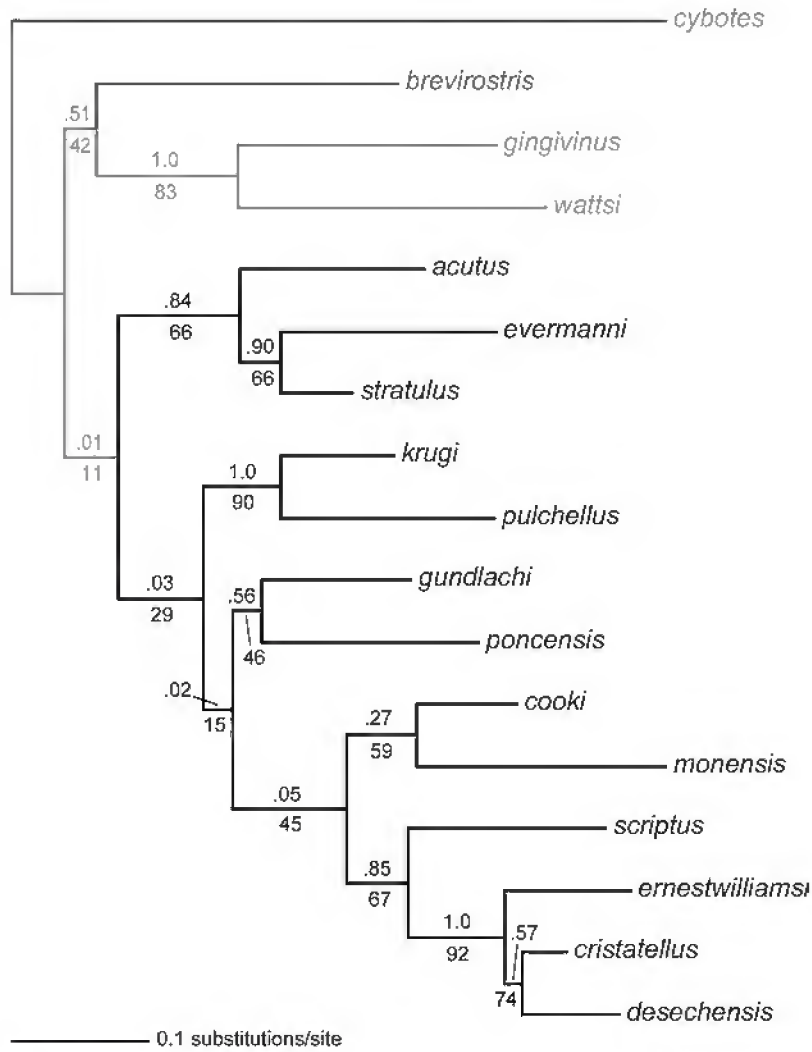

FIG. 7.—Maximum likelihood rooted phylogram for the cytochrome *b* mtDNA data set. Numbers above branches are "posterior probabilities," numbers below branches are likelihood bootstrap percentages. Outgroup taxa are shaded in light grey and the distichoids in medium grey.

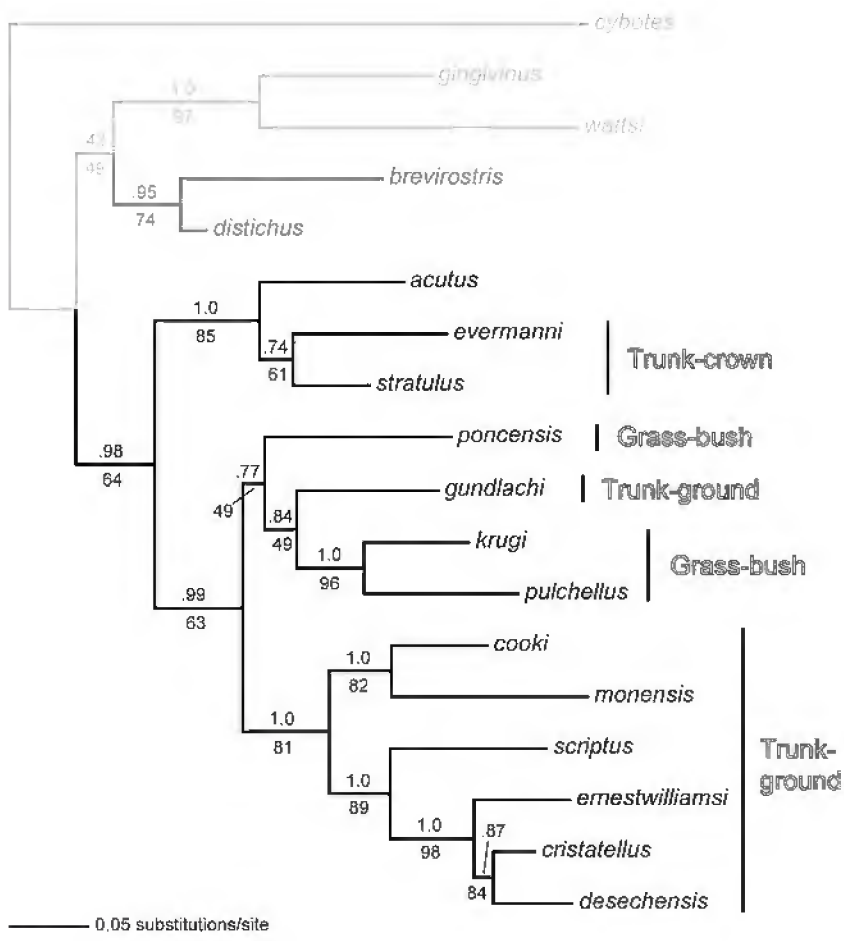

FIG. 8.—Maximum likelihood rooted phylogram of the combined 12S rRNA and cytochrome *b* data set. Numbers above branches are "posterior probabilities," numbers below branches are bootstrap percentages. This topology is also favored by the combined (summed) likelihood anaysis of mtDNA, morphological, and allozyme data (Table 5) as well as the mixed-model Bayesian analysis of the combined mtDNA and morphological data and is therefore our preferred phylogenetic hypothesis. The ecomorph status of each clade is shown to the right. Outgroup taxa are shaded in light grey and the distichoids in medium grey.

TABLE 3.—GTR+I+Γ model parameter values used in the maximum likelihood analyses of the separate and combined DNA data sets.

		Base frequencies				Substitution rates						Rate heterogeneity	
Data set	ln L	A	C	G	T	A ↔ C	A ↔ G	A ↔ T	C ↔ G	C ↔ T	G ↔ T	Γ	I
12S	−1414.6175	0.3799	0.1959	0.1776	0.2466	0.7708	7.4419	2.2359	0.0127	14.9306	1	0.6103	0.5091
cyt *b*[1]	−4925.8127	0.3009	0.2928	0.1136	0.2927	1.7655	12.0514	2.6603	1.1641	17.0250	1	1.5886	0.5396
cyt *b*[2]	−4651.0154	0.2998	0.2928	0.1141	0.2933	1.7391	12.9745	2.6950	1.2986	17.7324	1	1.8323	0.5499
mtDNA[3]	−6139.1713	0.3257	2.573	0.1396	0.2774	1.9084	11.6723	3.1890	0.8870	22.4751	1	1.0697	0.5555

[1] Parameters used in the analysis including *A. carolinensis* as an additional outgroup.
[2] Parameters estimated from the cyt *b* topology after removing *A. carolinensis*.
[3] Combined 12S and cyt *b* data sets.

TABLE 4.—Results of the SH tests for examining the congruence of the optimal topologies for particular data sets with alternative data sets. *P* values marked in bold are significant for $\alpha = 0.05$, indicating that the topology in question is a significantly worse explanation for the data set under consideration. The tree and data of the second allozyme data set is not included in the array of alternative topologies because doing so would require the elimination of many taxa from all data sets and trees and thus severely reduce the explanatory power of the analysis.

Dataset	Alternative topology	SH ($P =$)
Morphology		
	12S	**<0.001**
	cyt *b*[1]	**<0.001**
	mtDNA	**<0.001**
12S		
	Morphology	**<0.001**
	cyt *b*[1]	0.342
	mtDNA	0.767
cyt *b*		
	Morphology[2]	**<0.001**
	12S[2]	0.482
	mtDNA[2]	0.537
mtDNA		
	Morphology	**<0.001**
	12S	0.260
	cyt *b*[1]	0.361

[1] *A. distichus* removed from dataset.
[2] *A. distichus* removed from tree.

species. The remaining trunk-ground species form a strongly (*PP* = 0.99) to weakly (*LBP* = 60%) supported clade. The relationships within this clade exhibit weak support, with the exception of the relationship between *A. monensis* and *A. cooki* (*LBP* = 83%, *PP* = 0.98).

Cyt b.—Of 633 sites, 264 were variable and 229 parsimony-informative. Only a partial cyt *b* sequence was obtained for *A. acutus*, and none was obtained from *A. distichus*. For each successive likelihood search, the LRT selected the GTR+I+Γ (final parameter estimates in Table 3). model. In the resulting tree, the outgroup *A. cybotes* attached to *A. monensis*. This result is extremely suspicious and is in very strong conflict with essentially every past analysis of the *cristatellus* series. To assess the robustness of this result, we conducted an analysis including *A. carolinensis* as an additional outgroup (12S data from GenBank AF339050; Cyt *b* data provided by J. Losos) using the same model-testing and tree search methodology used for all other ML analyses. The resulting tree (ln *L* = –4925.8127) is topologically identical to the original analysis with the exception that *A. cybotes* now attaches to the branch between the *bimaculatus* series + distichoid clade and all other taxa (Fig. 7). Given these results, the placement of *A. cybotes* in the original analysis appears to be in error. Thus, all subsequent discussion of the cyt *b* tree and associated log-likelihoods and congruence tests will be in reference to the ML tree including *A. carolinensis*, but with *A. carolinensis* subsequently pruned from the topology. All bootstrap and Bayesian analyses were conducted without *A. carolinensis*. The Bayesian analyses reached stationarity at similar ln *L* scores (≈–4720) and supported the same overall tree (with the outgroup *A. cybotes* attaching to *A. monensis*). Posterior probabilities were calculated from 36,000 trees sampled at stationarity.

The distichoid *A. brevirostris* is weakly placed (*LBP* = 42%, *PP* = 0.51) as the sister taxon to the *bimaculatus* series. Support for the monophyly of the *cristatellus* series is weak (*LBP* = 11%, *PP* = 0.01). The basal division within this group is between a clade of trunk-crown anoles + *A. acutus* (*LBP* = 66%, *PP* = 0.84) and a clade of grass-bush + trunk-ground anoles (*LBP* = 29%, *PP* = 0.03). In contrast with the results based on several other data sets, the grass-bush species and *A. gundlachi* do not form a monophyletic group, but the alternative relationships of *A. gundlachi* and *A. poncensis* are poorly supported (*LBP* = 15%; *PP* = 0.02). The clade comprised of *A. krugi* and *A. pulchellus* is moderately (*LBP* = 90%) to strongly (*PP* = 1.0) supported and represents one branch of the basal divergence in the grass-bush + trunk-ground clade. The weakly supported clade of *A. poncensis* and *A. gundlachi* (*LBP* = 46%; *PP* = 0.56) is sister to a poorly supported (*LBP* = 45%, *PP* = 0.05) clade of trunk-ground species exclusive of *A. gundlachi*. The relationships within this clade are all weakly supported with the exception of the clade of *A. ernestwilliamsi*, *A. cristatellus*, and *A. desechensis* (*LBP* = 92%; *PP* = 1.0). It should be noted that the weak support for nested clades containing *A. monensis* is due to the Bayesian and ML bootstrap analyses mis-placing the root at the branch leading to that taxon (see above).

Combined 12S and cyt b.—The LRT again selected the GTR+I+Γ model for the com-

TABLE 5.—Summed likelihood scores for multiple data sets for the competing phylogenetic hypotheses. No cyt *b* data were obtained for *A. distichus*. The upper part of the table includes ln *Ls* calculated with *A. distichus* included in all data sets and trees, but coded as missing for the cyt *b* data and placed sister to *A. brevirostris* in the cyt *b* tree. The lower part of the table includes ln *Ls* calculated with *A. distichus* absent from all data sets. Taxon sampling in the second allozyme data set differs substantially from those of the other data sets; therefore, taxa unique to this data set were pruned from the tree and data set to make it comparable across trees. Characters of species for which no allozyme data were available were coded as missing. The tree of the second allozyme data set is not included in the array of alternative topologies because doing so would require the elimination of many taxa from all data sets and trees. Values for the morphological data tested on competing trees were calculated using the restricted maximum likelihood (REML) method implemented by PHYLIP v3.6a2.1. All other ln *Ls* were calculated using full likelihood in PAUP* 4b10. Total ln *Ls* sums closer to zero indicate better explanations of the data. The values in bold represent the best ln *L* for the particular data set or combination of data sets, and hence, the best explanation of the data set(s) in question.

	Topology			
Dataset	Morphology	12S	cyt *b*	Combined mtDNA
Anolis distichus included				
Morphology	**1420.2920**	1378.2287	1394.2805	1396.4772
12S	−1481.2427	**−1414.6175**	−1422.9215	−1415.5196
cyt *b*	−4737.6638	−4656.0301	**−4651.0154**	−4655.0195
Allozyme 2	**450.3723**	450.0681	448.8017	450.0681
Total	−4348.2422	−4242.3508	−4230.8547	**−4223.9938**
Anolis distichus excluded				
Morphology	**1305.9061**	1263.9600	1280.3425	1282.5320
12S	−1445.1977	**−1377.7052**	−1386.8032	−1378.8278
cyt *b*	−4737.6638	−4656.0301	**−4651.0154**	−4655.0195
Allozyme 2	**450.3723**	450.0681	448.8017	450.0681
Total	−4426.5831	−4319.7073	−4308.6744	**−4301.2472**

bined 12S and cyt *b* data set (hereafter called the mtDNA data set). A likelihood search using parameters in Table 3 inferred one tree with a ln $L = -6139.1713$ (Fig. 8). All Bayesian analyses attained stationarity at a similar ln *L* (≈−6161) and supported the same tree. Posterior probabilities were calculated from 36,000 trees sampled at stationarity. The tree is generally well-supported and is identical to the 12S tree with the exception of the placement of the distichoids and *A. acutus*, and to the cyt *b* except the placement of the *A. gundlachi* and *A. poncensis*. As with the analyses of the individual gene fragments, the placement of the distichoids is weakly supported.

Incongruence Among the Data Sets

There is one case in which topologies estimated from different data sets moderately or strongly support (*LBP* ≥ 70%) conflicting placements of taxa. The morphological tree places *A. poncensis* as the sister taxon of *A. pulchellus* (*LBP* = 77%); in contrast, the cyt *b* and combined mtDNA topologies strongly support *A. pulchellus* as the sister of *A. krugi*.

The morphological tree is a significantly worse explanation of all the other data sets (Table 4) according to the SH test. This tree is the only tree that places *A. gingivinus* and *A. wattsi* within the ingroup, the trunk anoles sister to the trunk-crown anoles, *A. acutus* with the grass-bush + trunk-ground clade, *A. pulchellus* and *A. poncensis* as sister taxa, and does not place *A. monensis* and *A. cooki* as sister taxa. The morphological tree also differs from the 12S, cyt *b*, and combined mtDNA topologies regarding the weakly supported relationships among the species *A. cristatellus*, *A. desechensis*, *A. ernestwilliamsi*, and *A. scriptus*. Conversely, the topologies inferred from the 12S, cyt *b* and combined mtDNA analyses are significantly worse explanations of the morphological data than is the morphological topology. The trees derived from the 12S, cyt *b* and combined mtDNA data sets are not significantly worse explanations for the alternative DNA data sets, which is not surprising given that the differences between the trees are relatively minor and not strongly supported.

Combined Analysis

The second allozyme tree was not included among the tested trees in the likelihood summing analysis because it lacks many taxa present in the DNA and morphological data set. To make the DNA and morphological trees comparable to the allozyme tree would necessitate the exclusion of many taxa from the corresponding data sets and thus reduce the explanatory power of the combined analyses. However, the second allozyme data set was used in the summed likelihood analysis. The combined mtDNA tree was also used. Two different analyses based on summed likelihoods were conducted to deal with the fact that *A. distichus* was not included in the cyt *b* data set. In the first, *A. distichus* was removed from all data sets and trees (the distichoids were still represented by the closely related *A. brevirostris*). In the second analysis, *A. distichus* was added to the cyt *b* tree as the sister taxon to *A. brevirostris*, a relationship that is strongly supported by the morphological and 12S analyses. These measures were necessary because when summing the log-likelihoods of the different data sets on competing trees, the sum of the cyt *b* tree would have been inflated relative to those of other trees simply because fewer taxa were used in calculating the summed ln *L*. Results of summing the likelihood scores for all the data sets on all relevant topologies are provided in Table 5. The mtDNA tree is the best explanation of the combined data whether *A. distichus* is included or excluded, followed by the cyt *b*, 12S, and morphology trees.

The mixed-model Bayesian analyses of the combined mtDNA and morphology data reached stationarity at a similar ln *L* (≈–6079) and supported the same topology. The consensus tree of 36,000 trees (not shown) is topologically identical to the combined mtDNA tree with the exception of the weakly supported relationship (*PP* = 0.46) of the distichoids sister to the *cristatellus* series. All other relationships are supported with a posterior probability ≥0.99 except the *A. gundlachi* + *A. krugi* + *A. pulchellus* clade (*PP* = 0.71).

Analyses of the Ancestral Ecomorph State and Estimated Times of Divergence

The ecomorph class of the ancestor that gave rise to the Puerto Rican *cristatellus* series radiation is ambiguous in the context of the combined mtDNA phylogeny; all of the ecomorph state assignments (trunk-crown, trunk-ground, and grass-bush) are equally parsimonious. The phylogenetic placement of each ecomorph class in the *cristatellus* series is provided on Fig. 8. The ultrametric tree inferred by the NPRS analysis, with nodes and branch lengths representing time is provided in Fig. 9; estimated divergence times are given in Table 6.

Discussion

Incongruence Among the Data Sets

The optimal topologies for the 12S, cyt *b*, and combined mtDNA data sets are significantly worse explanations of the morphological data than is the optimal topology for the morphological data set (Table 4). This indicates that although most of the nodes of the morphology tree are poorly supported, as a whole, the morphological data still strongly support an alternative phylogenetic history of the *cristatellus* series. If the tree favored by the combined analysis of morphological, mtDNA, and allozyme data sets (Table 5), is the best phylogenetic hypothesis (see below), then incongruence with the tree favored by the morphological data is due primarily to convergent evolution of some morphological characters (see "Morphological implications of the preferred tree").

The Phylogenetic History of the cristatellus *Series*

According to the sums of likelihood scores (Table 5), the mtDNA tree (i.e., the one resulting from analysis of the combined 12S and cyt *b* data) is the best estimate of the phylogeny for the combined mtDNA, morphological, and allozyme data. This result may be due to the fact that the mtDNA data set is much larger than the others and thus has a greater impact on the overall likelihood score, though a smaller data set that strongly favors one tree over another should have more influence on the final result than a larger data set that only weakly discriminates between the

trees. With the exception of the weakly supported sister relationship between the distichoids and the *cristatellus* series, the mtDNA tree is topologically identical to the consensus tree of the mixed-model Bayesian analyses of the mtDNA and morphology data. Consequently, we will treat the tree based on the combined mtDNA data (as well as the ingroup relationships of the combined mtDNA, morphology, and allozyme data) (Fig. 8) as the best estimate of the phylogeny for the *cristatellus* series. With the exception of the sister relationship between *A. poncensis* and *A. pulchellus*, this tree does not conflict with any of the moderately to well-supported nodes of the morphological tree and is congruent with many of the fixed or nearly fixed morphological characters (including karyotype). The three other moderately to well-supported nodes of the morphological tree are also well supported in the mtDNA tree. With the exception of the relationships of *A. pulchellus* and *A. poncensis*, the combined mtDNA tree is also congruent with all the moderately- to well-supported nodes in the trees based on all the other data sets. Incongruent relationships between the combined mtDNA tree and other analyses involve nodes that are not even moderately supported in the separate analyses. Finally, the mtDNA tree is topologically identical to a MANOB (parsimony) analysis of combined second allozyme, morphology, and mtDNA data sets (not shown) except for a weakly supported, conflicting placement of *A. acutus* as the sister of *A. evermanni*.

The tree that best explains the combined data (Fig. 8) is similar to past phylogenetic hypotheses of the *cristatellus* series. In particular, our results agree with the summary tree of Gorman et al. (1983:Fig. 6), based on analyses of allozyme and karyotypic data, in supporting the sister relationships of *A. stratulus* with *A. evermanni*, *A. cristatellus* (and *A. scriptus*) with *A. cooki* (and *A. monensis*), *A. pulchellus* with *A. krugi*, and *A. gundlachi* with the grass-bush species. Our results stongly support the relationships of *A. acutus*, a taxon whose phylogenetic affinities were ambiguous in the earlier study, with the trunk-crown anoles *A. evermanni* and *A. stratulus*. The morphological data place *A. acutus* as the sister taxon to the grass-bush + trunk-ground clade. *Anolis acutus* shares with this clade a distinct tail crest (character 19), keeled ventral scales (15), and the derived condition of the splenial overlap of the coronoid (31). However, the tail crest is absent in the grass-bush species, keeled ventrals are variably present in the grass-bush + trunk ground clade, and *A. stratulus* and *A. evermanni* lack splenials and therefore were not scored for character 31. The 12S, cyt *b*, and combined mtDNA, in contrast, support the placement of *A. acutus* with the trunk-crown anoles, *A. evermanni* and *A. stratulus* (*LBP* = 66–85%, *PP* = 0.86–0.99). Although not classified into any recognized ecomorph, *A. acutus* is morphometrically most similar to the trunk-crown anoles (Losos and de Queiroz, 1997).

One notable conflict with past studies is the placement of *A. gundlachi* and *A. poncensis* relative to the other grass-bush species. Gorman et al. (1983) placed *A. gundlachi* sister to a clade composed of the three grass-bush species. In contrast, our preferred tree places *A. gundlachi* nested within this grass-bush clade, however the combined mtDNA data cannot reject the hypothesis that the grass-bush anoles are monophyletic (SH test, $P = 0.184$).

The placement of the Hispañolan and Bahamian distichoids relative to the *bimaculatus* and *cristatellus* groups is not well supported. Nevertheless, in contrast with earlier hypotheses (e.g., Gorman et al., 1980, 1983), our results indicate that the distichoids are not particularly closely related to *A. acutus*, *A. evermanni*, and *A. stratulus*, nor are they nested within the *cristatellus* series (here defined as the clade stemming from the most recent common ancestor of *A. cristatellus*, *A. pulchellus*, *A. evermanni*, and *A. stratulus*). However, the combined mtDNA data cannot reject the hypothesis that the distichoids form a clade with *A. acutus*, *A. evermanni*, and *A. stratulus* ($P = 0.07$), nor the hypothesis that the distichoids are sister to the *cristatellus* series ($P = 0.49$).

The Evolution of Ecomorphs on Puerto Rico

The ecomorph class that represents the ancestral state for the *cristatellus* series is ambiguous. Part of this uncertainty results from the ecomorph status of *A. acutus* (close to, but not classifiable as, a trunk-crown species). However, even if *A. acutus* is considered a trunk crown species, the ancestral ecomoph is ambiguous. Because of this ambiguity, we cannot rule out the hypothesis that the ancestor of the *cristatellus* series was a member of the trunk-crown ecomorph or possessed a generalized body plan similar to that of *A. acutus* (Losos and de Queiroz, 1997). These alternatives are difficult to distinguish. Of the various ecomorphs, the trunk-crown ecomorph is the most similar to a hypothesized generalist body plan (Losos and de Queiroz, 1997). In addition, *A. acutus* (which inhabits St. Croix) occurs in a species-poor fauna and thus may not be subject to the same conditions that favor the evolution or maintenance of ecomorphs. Thus, *A. acutus* may possess the same ecomorph condition as it did when it split from the common ancestor of the Puerto Rican members of the *cristatellus* series, or else it may have evolved away from the trunk-crown ecomorph after colonizing a species-poor island.

Although we cannot unequivocally determine the ancestral ecomorph of the *cristatellus* series, we can infer, based on our best phylogenetic hypothesis, some things about the pattern of ecomorph evolution for the most inclusive crown clade containing the species that occur on Puerto Rico (i.e., the clade stemming from the most recent common ancestor of *A. evermanni*, *A. stratulus*, *A. poncensis*, *A. gundlachi*, *A. krugi*, *A. pulchellus*, *A. cooki*, and *A. cristatellus*). Our phylogenetic tree (Fig. 8) supports the hypothesis that the most basal divergence within this clade was between a lineage that gave rise to the present trunk-crown anoles (*A. evermanni* and *A. stratulus*) along with *A. acutus* and a second lineage that later radiated into the present grass-bush and trunk-ground species. The placement of *A. gundlachi* within the grass-bush clade suggests that either this species independently (i.e., relative to the clade made up of the other trunk-ground species) evolved a trunk-ground morphology from a grass-bush ancestor, or that the grass-bush morphology evolved independently in *A. poncensis* and in the ancestor of *A. krugi* and *A. pulchellus* from a trunk-ground ancestor. If patterns of ecomorph evolution are similar on different Greater Antillean islands (Losos, 1992), then the presence of trunk-ground anoles and absence of grass-bush anoles on Jamaica (Williams, 1983), and the inferred derivation of grass-bush anoles from trunk-ground anoles in the *sagrei* series of Cuba (based on the tree of Jackman et al., 1999) favor the latter scenario.

Morphological Implications of the Preferred Tree

Accepting the tree that best explains the combined mtDNA, morphology, and allozyme data as the best estimate of *Anolis cristatellus* series phylogeny has several implications for morphological evolution within the group, including several instances of convergent evolution. The morphological data support the sister relationship between the two most highly modified grass-bush species *A. poncensis* and *A. pulchellus*. Besides similar overall appearance, including the striped color pattern, slender body, and long tail characteristic of the grass bush ecomorph (also present, though sometimes to a lesser degree, in *A. krugi*), these taxa share enlargement of the dorsal scales (not coded as a separate state) as well as reduced toepads. If the grass-bush species were derived from trunk-ground ancestors (see previous section), then the preferred tree suggests that these characters arose independently in the lineages leading to the two species after they diverged from a common ancestor. Similarly, the placements of *A. acutus* and *A. gundlachi* imply that a tail crest has been gained or lost no less than three times. Keeled head scales appear to have arisen independently in the ancestor to the grass-bush + *A. gundlachi* clade as well as in *A. monensis* (the most parsimonious explanation), or to have evolved in the common ancestor to the trunk-ground + grass-bush clade and subsequently been lost twice. Finally, the *krugi*-type dentary sculpturing evolved in the common ancestor to the clade containing *A. gundlachi*, *A. krugi*, and *A. pulchellus* and independently in *A. monesis*. Lizards that possess the *krugi* type of sculp-

TABLE 6.—Divergence times (in millions of years) with 95% confidence intervals estimated by the NPRS analysis. The left side of the table represents estimated times with the basal divergence of the *cristatellus* series fixed to 8 MYA and the right to 16 MYA. Letters identify nodes in Fig. 9.

Node	8 MYA			16 MYA		
	Estimated Age	Lower 95% CI	Upper 95% CI	Estimated Age	Lower 95% CI	Upper 95% CI
A	10.2	10.0	10.4	20.3	19.8	21.2
B	9.1	9.0	9.3	18.2	17.7	18.9
C	5.7	5.5	5.8	11.3	10.7	12.0
D	6.4	6.2	6.6	12.8	11.9	13.6
E	4.8	4.6	5.0	9.7	9.1	10.2
F	3.8	3.6	3.9	7.5	7.0	8.1
G	6.1	6.0	6.1	12.1	11.8	12.4
H	5.5	5.4	5.5	10.9	10.6	11.2
I	4.6	4.5	4.7	9.3	8.9	9.6
J	3.0	3.0	3.1	6.1	5.7	6.4
K	4.4	4.3	4.5	8.7	8.4	9.1
L	3.1	3.0	3.2	6.2	5.9	6.5
M	3.2	3.1	3.3	6.4	6.1	6.7
N	1.7	1.6	1.7	3.4	3.1	3.6
O	1.3	1.2	1.4	2.6	2.4	2.8

turing seem to pass through a *cristatellus* type stage, suggesting that convergence may occur via hypermorphosis.

Historical Biogeography of the Anolis cristatellus *Series*

Any inferences about the biogeographic history of the *Anolis cristatellus* series must be made without aid of a detailed fossil record. Amber-preserved anoles exist from the mid-Miocene of the Dominican Republic (Rieppel, 1980; de Queiroz et al., 1998; Polcyn et al., 2002), but these species are not closely related to the *cristatellus* series. Puerto Rican fossil remains for the *cristatellus* series are limited to late Pleistocene deposits and include remains of species resembling *A. cristatellus*, *A. evermanni*, and *A. krugi* (Pregill, 1981). These data suggest that anoles have existed in the Caribbean at least since the Miocene and that all three ecomorphs found in the Puerto Rican members of the *cristatellus* series were already established by the late Pleistocene. Due to the lack of pre-Pleistocene fossil evidence, our biogeographic hypotheses are based primarily on our best estimate of the phylogeny of the group (Fig. 8), recent interpretations of the geologic history of the region, and divergence dates inferred by the NPRS analysis (Table 6; Fig. 9). Unless otherwise noted, the following geological discussions rely primarily on the work of Iturralde-Vinent and MacPhee (1999) and references therein. The Puerto Rican island bank—which formed a single landmass when sea levels were lower during the Pleistocene and includes the island of Puerto Rico and most of the Virgin Islands, but not

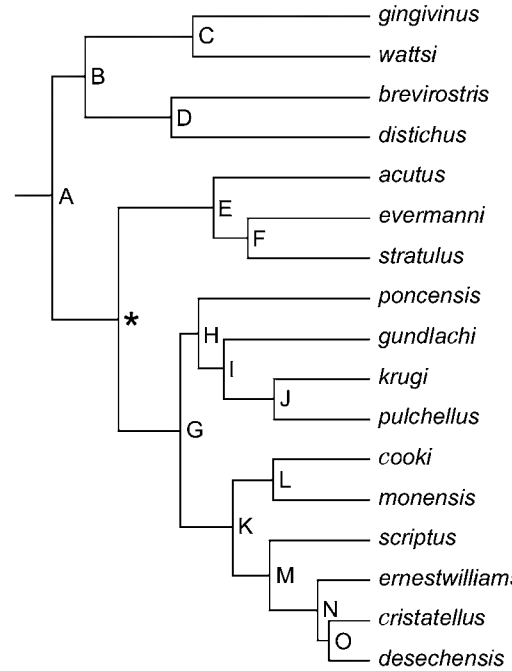

FIG. 9.—Chronogram inferred by the NPRS analysis. Branch lengths represent time. Node labels correspond to Table 6. The asterisk represents the node for which the age was fixed at 8 or 16 MYA.

the islands of St. Croix, Mona, Monita, or Desecheo (Heatwole and MacKenzie, 1967)—will be referred to simply as Puerto Rico in the following discussion. Because of the weakly supported relationships among the distichoids and the *bimaculatus* and *cristatellus* groups we restrict our biogeographical discussion to the members of the *cristatellus* series.

The presence of *A. acutus* on St. Croix is enigmatic. St. Croix has had no aerial connection to Puerto Rico since the Early Oligocene (33–35 MYA; Iturralde-Vinent and MacPhee, 1999) if ever. The dates inferred by the NPRS analysis suggest that *A. acutus* split from the common ancestor to *A. evermanni* and *A. stratulus* ~10 MYA. Thus, the isolation of this species on St. Croix is best explained by dispersal. Yet, the position of St. Croix to the southeast of Puerto Rico requires that the ancestor of *A. acutus* disperse against the prevailing east-west sea current. Although these currents generally flow east to west, experiments of satellite-tracked, free-floating buoys (Molinari et al., 1979) have demonstrated that a floating object does not necessarily follow an unaltered east-west journey. Rather, it is subject to local conditions such as cyclonic circulation or storms (Molinari et al., 1979; Kinder, 1983; Kinder et al. 1985; Sou et al., 1996; see Fig. 11A, Itturalde-Vinent and MacPhee, 1999). Therefore, local current conditions could possibly permit debris from Puerto Rico to reach nearby islands not immediately downstream. Hurricanes may provide another mechanism allowing dispersal of the ancestor of *A. acutus* to St. Croix. This phenomenon has been documented recently with the dispersal of multiple specimens of *Iguana iguana* to Anguilla from islands further south (Censky et al., 1998). Although currently, high-energy storms generally travel southeast to northwest, changes in the Circumtropical Current during the Mid to Late Miocene, if they existed, could have deflected these storms southward (Iturralde-Vinent and MacPhee, 1999).

A combination of vicariance due to Pliocene or Pleistocene changes in sea level and overwater dispersal on prevailing currents best explain the distribution of the *cristatellus* series taxa that currently inhabit the Virgin Islands (other than St. Croix) and satellite islands of Puerto Rico. During periods of maximum glaciation, sea levels in the Caribbean were as much as 160 m lower than the present level (Donn et al., 1962). As a consequence, Puerto Rico and the Virgin Islands (except St. Croix) formed a single exposed landmass. As sea levels rose, they subsequently fragmented that landmass (Heatwole and Mackenzie, 1967) and isolated populations of widespread species, including *A. pulchellus*, *A. stratulus*, and *A. cristatellus*, on a number of different islands in this group. The isolation and subsequent evolution of large body size of an *A. cristatellus* population on one of the small cays known as Carrot Rock resulted in the currently recognized *A. ernestwilliamsi* (Lazell, 1983). It should be noted that *A. cristatellus* is a widespread taxon that exhibits substantial genetic substructure (R. Glor, personal communication), while *A. ernestwilliamsi* is a small, allopatric population that is likely most closely related to nearby populations of *A. cristatellus* in the Virgin Islands. Given that our sample of *A. cristatellus* is from the north central part of the main island of Puerto Rico, its divergence from *A. ernestwilliamsi* on Carrot Rock (Fig. 9) and estimated divergence date (~1.7–3.6 MYA) is likely greater than that for geographically more proximate populations of *A. cristatellus* in the Virgin Islands.

The prevailing southeast to northwest sea current has likely remained unchanged since the appearance of the Panamanian land bridge at the end of the Pliocene (Iturralde-Vinent and MacPhee, 1999). This current would bring debris from the Puerto Rican Island bank to islands off the western shore (Desecheo, Mona, Monita), where *A. desechensis* and *A. monensis* now occur, as well as to the Bahamas, which are currently inhabited by *A. scriptus* (Heatwole and MacKenzie, 1967; Williams, 1969). The ability of animals to survive on floating debris in the Caribbean is well documented (Heatwole and Levins, 1972; Censky et al., 1998).

The well-supported sister relationship of *A. monensis* and *A. cooki* suggests that Mona and Monita were colonized by *A. cooki* or a common ancestor. Although geological information about these islands is scarce, they are composed of limestone and hypothesized to have been uplifted sometime in the Miocene and not previously connected to Puerto Rico

(Kaye, 1959). Given that *A. cooki* is restricted to the southwestern portion of Puerto Rico and that ocean currents lead directly from this region to the vicinity of Mona and Monita (see above), the occurrence of *A. monensis* on those islands is best explained by over water dispersal (Williams, 1969). As in the case of *A. cristatellus* and *A. ernestwilliamsi*, the age of the split between *A. cooki* and *A. monensis* (~3.2–6.5 MYA) may be overestimated. Although *A. cooki* is not nearly as widely distributed as is *A. cristatellus*, our sample of *A. cooki* is from the central part of the distribution of the species, while the most likely source of colonists for Mona and Monita is farther to the west. If *A. cooki* exhibits geographically structured mtDNA haplotypes, then samples of western *A. cooki* may exhibit smaller levels of divergence from *A. monensis*, implying a more recent divergence time.

It has been suggested that the Bahamas were submerged prior to 65,000 years ago (Alt and Brooks, 1965). If true, the isolation of *A. scriptus* in the Bahamas must have occurred since that time. Yet, our estimate for the divergence of this taxon relative to *A. cristatellus*, *A. ernestwilliamsi*, and *A. desechensis* is much older (~3.3–7.6 MYA). This discrepancy may be explained simply as a gene tree split rather than a species split (similar to the cases of *A. ernestwilliamsi* and *A. monensis*, above). Alternatively, a Bahamian landmass may have remained continually aerial during periods of maximum sea level or was colonized via some geographically intermediate landmass on which the ancestral population is now extinct (as postulated to explain a similar phenomenon for the Galápagos iguanas [Rassman, 1997]). Given that the Bahamas and Puerto Rico have not been physically connected any time since the break-up of Hispañola and Puerto Rico, the occurrence of *A. scriptus* in the Bahamas can only be explained by dispersal. In addition, *A. scriptus* is restricted to the southeastern-most islands in the archipelago (Schwartz and Henderson, 1991), which are the same islands that would most likely be colonized from Puerto Rico via ocean currents.

What little geologic information exists for Isla Desecheo indicates that it is not part of the Puerto Rico landmass and likely became aerial some time during the Pleistocene, remaining emergent since (Seiders et al., 1972). The island is only 21 km offshore of Puerto Rico and in the direct path of ocean currents from that landmass. Thus, dispersal from a mainland population of *A. cristatellus* is probable. Once again, the estimated divergence between *A. cristatellus* and *A. desechensis* (~1.4–2.8 MYA) is likely overestimated given that our sample of the former species in from north central Puerto Rico while the most likely source of colonists is the eastern part of the island. We can nonetheless infer that the isolation of *A. desechensis* is a relatively recent event.

Taxonomy

The relationships inferred in this study (Fig. 8) have implications for the taxonomy of the *cristatellus* and *bimaculatus* series, and we therefore propose a revised taxonomy for those groups. Several studies have indicated a close relationship between the *cristatellus* and *bimaculatus* series (e.g., Etheridge, 1959; Jackman et al., 1999; Poe, 2004). We apply the name *Ctenonotus* to this putative clade, not as a genus name (Guyer and Savage, 1987), but as the name of a subclade of the larger clade *Anolis*. No formal definition is proposed for *Ctenonotus*, but the name is applied to the least inclusive clade containing *A. bimaculatus*, *A. wattsi*, *A. distichus*, *A. cristatellus*, and *A. evermanni*. Subclades of *Ctenonotus* are given informal names composed of the specific epithet of the earliest named included species combined with one or more terms traditionally used as taxonomic ranks between genus and species (series, subseries, species group, and superspecies), following Etheridge (1959), Williams (1976), and many subsequent authors. In our taxonomy, however, these terms are not used as taxonomic ranks but simply as parts of the informal clade names. Nevertheless, these terms are used in a way that maintains their traditional hierarchical relationships (e.g., the *cristatellus* series includes the *cristatellus* subseries which includes the *cristatellus* species group). Otherwise, these terms are, for the most part, used arbitrarily (e.g., the *acutus* subseries could just as well have been the *acutus* species group). One exception is that we have reserved use of the term "superspecies" for clades composed of species

all of which are mutually allopatric. Lists of terminal species within the smallest named clades begin with the species upon whose name the name of the clade is based. The remaining species are listed alphabetically (as opposed to being sequenced in order of phylogenetic branching). Because relationships of the distichoids remain uncertain, they are placed in their own series, following Burnell and Hedges (1990). Because our study focuses on the *cristatellus* series, subclades and lists of included species are given only for that series. For species included in the *bimaculatus* and *distichus* series, see Burnell and Hedges (1990), except that *A. eugenegrahami* is excluded from the *distichus* series (Williams, 1989).

Ctenonotus Fitzinger 1843
- *bimaculatus* series
- *distichus* series
- *cristatellus* series
  - *acutus* subseries
    - *A. acutus* Hallowell 1856
    - *A. evermanni* Stejneger 1904
    - *A. stratulus* Cope 1861
  - *cristatellus* subseries
    - *cristatellus* species group
      - *cristatellus* superspecies
        - *A. cristatellus* Duméril and Bibron 1837
        - *A. desechensis* Heatwole 1976
        - *A. ernestwilliamsi* Lazell 1983
        - *A. scriptus* Garman 1887
      - *monensis* superspecies
        - *A. monensis* Stejneger 1904
        - *A. cooki* Grant 1931
    - *pulchellus* species group
      - *A. pulchellus* Duméril and Bibron 1837
      - *A. gundlachi* Peters 1876
      - *A. krugi* Peters 1876
      - *A. poncensis* Stejneger 1904

Acknowledgments.—This study fulfills one of MCB's requirements for a bachelor's degree at the University of Oklahoma, and for participation in the Research Training Program at the National Museum of Natural History. We sincerely thank P. Kores and M. Molvray for their advice and resources, without which portions of the molecular portion of this project would have been impossible. We also thank R. Glor, J. Lazell, J. Losos, G. Mayer, and the LSU Museum of Natural Science Collection of Genetic Resources for providing tissue samples; J. Rosado and the MCZ, and G. Schneider and the UMMZ for specimen loans; M. Braun and the Laboratory of Molecular Systematics, Smithsonian Institution, J. Caldwell, J. McGuire, T. Reeder, D. Swofford, L. Vitt, and J. Wilgenbusch for facility use for data collection, analysis and manuscript preparation; R. Broughton, L. Young, and N. Zehrbach for assistance and guidance with lab work; J. Wilgenbusch for providing primers; R. Etheridge for access to his data; C. Gordon and L. García Pérez for data collection; M. Sangrey and the Research Training program at the National Museum of Natural History; K. Tighe for radiograph assistance; D. Brandley and J. Panek for lodging during portions of this study; T. Devitt, W. Fair, J. Felsenstein, M. Fujita, A. Leaché, J. McGuire, G. Pregill, J. Savage, J. Wiens, J. Wilgenbusch, and one anonymous reviewer for helpful advice and/or comments on the manuscript; R. Glor for helpful discussions about the intraspecific phylogeny of *A. cristatellus*; J. Huelsenbeck for an unreleased beta version of MrBayes, and A. Seago for figures 10–13. D. Warren provided a Perl script that greatly aided in conducting the g_1 simulations as well as providing a beta copy of Converge v0.1. Funding was provided by a University of Oklahoma Undergraduate Research Opportunities Program grant awarded to MCB; NSF DEB 9982736 awarded to J. Losos, KdQ, and A. Larson; and a National Science Foundation Research Experiences for Undergraduates Program grant, DBI-9820303, awarded to the Research Training Program at the National Museum of Natural History. We thank the Departamento de Recursos Naturales, Puerto Rico (No. DRN-92-75); the Departamento de Vida Silvestre, Republica Dominica (No. 413/91); and the Ministry of Agriculture, Fisheries, Lands, and Housing, Antigua (No. AFLH 22/40) for issuing permits.

Literature Cited

Alt, D., and H. K. Brooks. 1965. Age of Florida marine terraces. Journal of Geology 73:406–411.

Archie, J. W. 1989. A randomization test for phylogenetic information in systematic data. Systematic Zoology 38:219–252.

Arnold, D. L. 1980. Geographic variation in *Anolis brevirostris* (Sauria: Iguanidae) in Hispaniola. Breviora 461:1–31.

Berlocher, S. H., and D. L. Swofford. 1997. Searching for phylogenetic trees under the frequency parsimony criterion: an approach using generalized parsimony. Systematic Biology 46:211–215.

Beuttell, K., and J. B. Losos. 1999. Ecological morphology of Caribbean anoles. Herpetological Monographs 13:1–28.

Burnell, K. L., and S. B. Hedges. 1990. Relationships of West Indian *Anolis* (Sauria: Iguanidae): an approach using slowly-evolving protein loci. Caribbean Journal of Science 26:7–30.

Censky, E. J., K. Hodge, and J. Dudley. 1998. Over-water dispersal of lizards due to hurricanes. Nature 395:556.

Creer, D. A., K. de Queiroz, T. R. Jackman, J. B. Losos, and A. Larson. 2001. Systematics of the *Anolis roquet* series of the southern Lesser Antilles. Journal of Herpetology 35:428–441.

DE QUEIROZ, K. 1987. Phylogenetic systematics of iguanine lizards: a comparative osteological study. University of California Publications in Zoology 118:1–203.

DE QUEIROZ, K., L.-R. CHU, AND J. B. LOSOS. 1998. A second *Anolis* lizard in Dominican amber and the systematics and ecological morphology of Dominican amber anoles. American Museum Novitates 3249:1–23.

DONN, W. L., W. R. FARRAND, AND M. EWING. 1962. Pleistocene ice volumes and sea-level lowering. Journal of Geology 70:206–214.

EDWARDS, A. W. F. 1970. Estimation of the branch points of a branching diffusion process. Journal of the Royal Statistical Society B 32:155–174.

———. 1972. Likelihood. Cambridge University Press, Cambridge, U.K. [Expanded edition published by Johns Hopkins University Press, Baltimore, Maryland, U.S.A., 1992.]

ETHERIDGE, R. 1959. The Relationships of the Anoles (Reptilia: Sauria: Iguanidae): An Interpretation Based on Skeletal Morphology. Ph.D. Dissertation, University of Michigan, Ann Arbor, Michigan, USA.

FAITH, D. P., AND P. S. CRANSTON. 1991. Could a cladogram this short have arisen by chance alone? On permutation tests for cladistic structure. Cladistics 7:1–28.

FELSENSTEIN, J. 1978. Cases in which parsimony and compatibility methods will be positively misleading. Systematic Zoology 27:401–410.

———. 1973. Maximum-likelihood estimation of evolutionary trees from continuous characters. American Journal of Human Genetics 25:471–492.

———. 1981. Evolutionary trees from gene frequencies and quantitative characters: finding maximum likelihood estimates. Evolution 35:1229–1242.

———. 1985. Phylogenies from gene frequencies: a statistical problem. Systematic Zoology 34:200–311.

———. 1988. Phylogenies and quantitative characters. Annual Reviews of Ecology and Systematics 19:445–471.

———. 1993. PHYLIP (Phylogeny Inference Package) version 3.6a2. Distributed by the author. Department of Genome Sciences, University of Washington, Seattle.

———. 2002. Quantitative characters, phylogenies, and morphometrics. Pp. 27–44. *In* N. MacLeod (Ed.), Morphology, Shape, and Phylogenetics. Systematics Association Special Volume Series 64. Taylor and Francis,London, England.

GORMAN, G. C. 1973. The chromosomes of the Reptilia, a cytotaxonomic interpretation. Pp. 349–424. *In* A. B. Chiarelli and E. Capanna (Eds.), Cytotaxonomy and Vertebrate Evolution. Academic Press, New York, New York, U.S.A.

GORMAN, G. C., R. THOMAS, AND L. ATKINS. 1968. Intra- and interspecific chromosome variation in *Anolis cristatellus* and its closest relatives. Breviora 293:1–12.

GORMAN, G. C., AND L. ATKINS. 1969. The Zoogeography of Lesser Antillean *Anolis* lizards—an analysis based upon chromosomes and lactic dehydrogenases. Bulletin of the Museum of Comparative Zoology 138:53–80.

GORMAN, G. C., D. G. BUTH, AND J. S. WYLES. 1980*a*. *Anolis* lizards of the Eastern Caribbean: a case study in evolution. III. A cladistic analysis of albumin immunological data, and the definition of species groups. Systematic Zoology 29:143–158.

GORMAN, G. C., D. BUTH, M. SOULÉ, AND S. Y. YANG. 1980*b*. The relationships of the *Anolis cristatellus* species group: electrophoretic analysis. Journal of Herpetology 14:269–278.

———. 1983. The relationships of the Puerto Rican *Anolis*: electrophoretic and karyotypic studies. Pp. 626–642. *In* A. G. J. Rhodin, and K. Miyata (Eds.), Advances in Herpetology and Evolutionary Biology. Museum of Comparative Zoology, Cambridge, Massachusetts, U.S.A.

GORMAN, G. C., AND R. B. STAMM. 1975. The *Anolis* lizards of Mona, Redonda, and La Blanquilla: chromosomes, relationships, and natural history notes. Journal of Herpetology 9:197–205.

GORMAN, G. C., AND Y. J. KIM. 1976. *Anolis* lizards of the eastern Caribbean: a case study in evolution. II. Genetic relationships and genetic variation of the *bimaculatus* group. Systematic Zoology 25:62–77.

GUYER, C., AND J. M. SAVAGE. 1986. Cladistic relationships among anoles (Sauria: Iguanidae). Systematic Zoology 35:509–531.

HASTINGS, W. K. 1970. Monte-Carlo sampling methods using Markov Chains and their applications. Biometrika 57:97–109.

HEATWOLE, H., AND F. MACKENZIE. 1967. Herpetogeography of Puerto Rico. IV. Paleogeography, faunal similarity and endemism. Evolution 21:429–438.

HEATWOLE, H., AND R. LEVINS. 1972. Biogeography of the Puerto Rican Bank: flotsam transport of terrestrial animals. Ecology 53:112–117.

HENDY, M. D., AND D. PENNY. 1989. A framework for the quantitative study of evolutionary trees. Systematic Zoology 38:297–309.

HICKSON, R. E., C. SIMON, A. COOPER, G. S. SPICER, J. SULLIVAN, AND D. PENNY. 1996. Conserved sequence motifs, alignment, and secondary structure for the third domain of animal 12S rRNA. Molecular Biology and Evolution 13:150–169.

HILLIS, D. M., AND J. P. HUELSENBECK. 1992. Signal, noise, and reliability in molecular phylogenetic analyses. Journal of Heredity 83:189–195.

HUELSENBECK, J. P. 1995. Performance of phylogenetic methods in simulation. Systematic Biology 44:17–48.

———. 1997. Is the Felsenstein zone a fly trap? Systematic Biology 46:69–74.

HUELSENBECK, J. P., AND F. RONQUIST. 2001. MRBAYES: Bayesian inference of phylogeny. Bioinformatics 17: 754–755.

ITURRALDE-VINENT, M., AND R. MACPHEE. 1996. Age and paleogeographical origin of Dominican amber. Science 273:1850–1852.

———. 1999. Paleogeography of the Caribbean region, implications for Cenozoic biogeography. Bulletin of the American Museum of Natural History 238:1–95.

JACKMAN, T., J. B. LOSOS, A. LARSON, AND K. DE QUEIROZ. 1997. Phylogenetic studies of convergent adaptive radiations in Caribbean *Anolis* lizards. Pp. 535–557. *In* T. J. Givnish and K. J. Sytsma (Eds.), Molecular Evolution and Adaptive Radiation. Cambridge University Press, Cambridge, U.K.

JACKMAN, T., A. LARSON, K. DE QUEIROZ, AND J. B. LOSOS. 1999. Phylogenetic relationships and tempo of early diversification in *Anolis* lizards. Systematic Biology 48:254–285.

Jackman, T. R., D. J. Irschick, K. de Queiroz, J. B. Losos, and A. Larson. 2002. Molecular phylogenetic perspective on evolution of lizards of the *Anolis grahami* series. Journal of Experimental Zoology 294:1–16.

Kaye, C. A. 1959. Geology of Isla Mona Puerto Rico, and notes on age of Mona Passage. Geological Survey Professional Paper 317-C. United States Government Printing Office, Washington, D.C., U.S.A.

Kinder, T. H. 1983. Shallow currents in the Caribbean Sea and the Gulf of Mexico as observed with satellite-tracked drifters. Bulletin of Marine Science 33:239–246.

Kinder, T. H., G. W. Heburn, and A. W. Green. 1985. Some aspects of Caribbean circulation. Marine Geology 68:25–52.

Kishino, H., and M. Hasegawa. 1989. Evaluation of the maximum likelihood estimate of the evolutionary tree topologies from DNA sequence data, and the branching order in Hominoidea. Journal of Molecular Evolution 29:170–179.

Kjer, K. M. 1995. Use of rRNA secondary structure in phylogenetic studies to identify homologous positions: an example of alignment and data presentation from the frogs. Molecular Phylogenetics and Evolution 4:314–330.

Kocher, T. D., W. K. Thomas, A. Meyer, S. V. Edwards, S. Pääbo, F. X. Villablanca, and A. C. Wilson. 1989. Dynamics of mitochondrial DNA evolution in animals—amplification and sequencing with conserved primers. Proceedings of the National Academy of Sciences U.S.A. 86:6196–6200.

Larget, B., and D. L. Simon. 1999. Markov chain Monte Carlo algorithms for the Bayesian analysis of phylogenetic trees. Molecular Biology and Evolution 16:750–759.

Lazell, J. D., Jr. 1983. Biogeography of the herpetofauna of the British Virgin Islands, with description of a new anole (Sauria: Iguanidae). Pp. 99–117. *In* A. G. J. Rhodin and K. Miyata (Eds.), Advances in Herpetology and Evolutionary Biology. Museum of Comparative Zoology, Cambridge, Massachusetts, U.S.A.

Leaché, A. D., and T. W. Reeder. 2002. Molecular systematics of the Eastern Fence Lizard (*Sceloporus undulatus*): a comparison of parsimony, likelihood, and Bayesian approaches. Systematic Biology 51:44–68.

Leviton, A. E., R. H. Gibbs, Jr., E. Heal, and C. E. Dawson. 1985. Standards in herpetology and ichthyology: part 1. Standard symbolic codes for institutional resource collections in herpetology and ichthyology. Copeia 1985:802–832.

Lewis, P. O. 2001. A likelihood approach to estimating phylogeny from discrete morphological character data. Systematic Biology 50:913–925.

Losos, J. B. 1990. Ecomorphology, performance capability, and scaling of West Indian *Anolis* lizards: an evolutionary analysis. Ecological Monographs 60:369–388.

———. 1992. The evolution of convergent structure in Caribbean *Anolis* communities. Systematic Biology 41:403–420.

———. 1994. Integrative approaches to evolutionary ecology—*Anolis* lizards as model systems. Annual Review of Ecology and Systematics 25:467–493.

Losos, J. B., and K. de Queiroz. 1997. Evolutionary consequences of ecological release in Caribbean *Anolis* lizards. Biological Journal of the Linnean Society 61:459–483.

Losos, J. B., T. R. Jackman, A. Larson, K. de Queiroz, and L. Rodríguez-Schettino. 1998. Contingency and determinism in adaptive radiations of island lizards. Science 279:2115–2118.

MacPhee, R. D. E., M. A. Iturralde-Vinent, and E. S. Gaffney. 2003. Domo de Zaza, an early Miocene vertebrate locality in South-Central Cuba, with notes on the tectonic evolution of Puerto Rico and the Mona Passage. American Museum Novitates 3394:1–42.

Maddison, W. P., and D. R. Maddison. 2000. MacClade version 4. Sinauer Associates, Sunderland, Massachusetts, U.S.A.

Metropolis, N., A. W. Rosenbluth, M. N. Rosenbluth, and A. H. Teller. 1953. Equations of state calculations by fast computing machines. Journal of Chemical Physics 21:1087–1091.

Molinari, R. L., D. K. Atwood, C. Duckett, M. Spillane, and J. Brooks. 1979. Surface currents in the Caribbean Sea as deduced from satellite tracked drifting buoys. Proceedings of the Gulf Caribbean Fisheries Institute 1979 :106–113.

Nicholson, K. E. 2002. Phylogenetic analysis and a test of the current infrageneric classification of *Norops* (beta *Anolis*). Herpetological Monographs 16:93–120.

Nylander J. A. A. 2002. MrModeltest v1.0b. Program distributed by the author. Department of Systematic Zoology, Uppsala University.

Oelrich, T. M. 1958. The anatomy of the head of *Ctenosaura pectinata* (Iguanidae). University of Michigan Museum of Zoology Miscellaneous Publication 94:1–122.

Pimentel, R. A., and R. Riggins. 1987. The nature of cladistic data. Cladistics 3:201–209.

Pindell, J. L., and S. F. Barrett. 1990. Geological evolution of the Caribbean region; a plate tectonic perspective. Pp. 405–432. *In* G. Dengo and J. E. Case (Eds.), The Geology of North America, Vol. H. The Caribbean region. Geological Society of America, Boulder, Colorado, U.S.A.

Poe, S. 1998. Skull characters and the cladistic relationships of the Hispaniolan dwarf twig *Anolis*. Herpetological Monographs 11:192–236.

Poe, S. 2004. Phylogeny of anoles. Herpetological Monographs 18:37–89.

Polcyn, M. J., J. V. Rogers II, Y. Kobayashi, and L. L. Jacobs. 2002. Computed tomography of an *Anolis* lizard in Dominican amber: systematic, taphonomic, biogeographic, and evolutionary implications. Palaeontologia Electronica 5:13pp.

Posada, D., and K. A. Crandall. 1998. Modeltest: testing the model of DNA substitution. Bioinformatics 14:817–818.

Pregill, G. 1981. Late Pleistocene Herpetofaunas from Puerto Rico. University of Kansas Museum of Natural History Miscellaneous Publication 71:1–72.

Rassmann, K. 1997. Evolutionary age of the Galápagos iguanas predates the age of the present Galápagos Islands. Molecular Phylogenetics and Evolution 7: 158–172.

Reeder, T. W. 1995. Phylogenetic relationships among phrynosomatid lizards as inferred from mitochondrial ribosomal DNA sequences: substitutional bias and information content of transitions relative to transversions. Molecular Phylogenetics and Evolution 4: 203–222.

Rieppel, O. 1980. Green anole in Dominican amber. Nature 286:486–487.

Sanderson, M. J. 1997. A nonparametric approach to estimating divergence times in the absence of rate constancy. Molecular Biology and Evolution 14: 1218–1231.

Savage, J. M., and C. Guyer. 1989. Infrageneric classification and species composition of the anole genera, *Anolis*, *Ctenonotus*, *Dactyloa*, *Norops*, and *Semiurus* (Sauria: Iguanidae). Amphibia-Reptilia 10:105–116.

Schneider, C. J., L. B. Losos, and K. de Queiroz. 2001. Evolutionary relationships of the *Anolis bimaculatus* group from the Northern Lesser Antilles. Journal of Herpetology 35:1–12.

Shochat, D., and H. C. Dessauer. 1981. Comparative immunological study of the albumins of *Anolis* lizards of the Caribbean Islands. Comparative Biochemistry and Physiology 68A:67–73.

Schwartz, A., and R. W. Henderson. 1991. Amphibians and reptiles of the West Indies: descriptions, distributions, and natural history. University of Florida Press, Gainesville, Florida, U.S.A.

Seiders, V. M., R. P. Briggs, and L. Glover III. 1972. Geology of Isla Desecheo, Puerto Rico, with notes on the Great Southern Puerto Rico Fault Zone and Quaternary stillstands of the sea. Geological Survey Professional Paper 739. United States Government Printing Office, Washington, D.C., U.S.A.

Shimodaira, H., and M. Hasegawa. 1999. Multiple comparisons of log-likelihoods with applications to phylogenetic inference. Molecular Biology and Evolution 16:1114–1116.

Sou, T., G. Halloway, and M. Eby. 1996. Effect of topographic stress on Caribbean Sea circulation. Journal of Geophysical Research 101(C7):16,449–16,453.

Stevens, P. F. 1991. Character states, morphological variation, and phylogenetic analysis: a review. Systematic Biology 50:156–169.

Swofford, D. L. 2002. PAUP*. Phylogenetic Analysis Using Parsimony (*and Other Methods), version 4. Sinauer Associates, Sunderland, Massachusetts, U.S.A.

Swofford, D. L, and S. H. Berlocher. 1987. Inferring evolutionary trees from gene frequency data under the principle of maximum parsimony. Systematic Zoology 36:293–325.

Swofford, D. L., G. J. Olsen, P. J. Waddell, and D. M. Hillis. 1996. Phylogenetic inference. Pp. 407–543. *In* D. M. Hillis, C. Moritz, and B.K. Mable (Eds.), Molecular Systematics, 2nd ed. Sinauer Associates, Sunderland, Massachusetts, U.S.A

Tamura, K., and M. Nei. 1993. Estimation of the number of nucleotide substitutions in the control region of mitochondrial DNA in humans and chimpanzees. Molecular Biology and Evolution 10:512–526.

Thompson, J. D., T. J. Gibson, F. Plewniak, F. Jeanmougin, and D. G. Higgins. 1997. The ClustalX windows interface: flexible strategies for multiple sequence alignment aided by quality analysis tools. Nucleic Acids Research 24:4876–4882.

Titus, T. A., and D. R. Frost. 1996. Molecular homology assessment and phylogeny in the lizard family Opluridae (Squamata: Iguania). Molecular Phylogenetics and Evolution 6:49–62.

Warren, D. L., J. Wilgenbusch, and D. L. Swofford. 2003. Converge: A program for implementing MCMC convergence diagnostics. Available from the authors at danwarren@ucdavis.edu.

Wiens, J. J. 1995. Polymorphic characters in phylogenetic systematics. Systematic Biology 44:482–500.

———. 1998. Testing phylogenetic methods with tree-congruence: phylogenetic analysis of polymorphic morphological characters in phrynosomatid lizards. Systematic Biology 47:411–428.

———. 1999. Polymorphism in systematics and comparative biology. Annual Review of Ecology and Systematics 30:327–362.

———. 2000. Coding morphological variation for phylogenetic analysis: analyzing polymorphism and interspecific variation in higher taxa. Pp. 115–145. *In* J. J. Wiens (Ed.), Phylogenetic Analysis of Morphological Data. Smithsonian Institution Press, Washington, D.C., U.S.A.

———. 2001. Character analysis in morphological phylogenetics: problems and solutions. Systematic Biology 50:689–699.

Wiens, J. J., and T. W. Reeder. 1997. Phylogeny of the spiny lizards (*Sceloporus*) based on molecular and morphological evidence. Herpetological Monographs 11:1–101.

Wiens, J. J., and M. R. Servedio. 1997. Accuracy of phylogenetic analysis including and excluding polymorphic characters. Systematic Biology 46:332–345.

———. 1998. Phylogenetic analysis and intraspecific variation: performance of parsimony, likelihood, and distance methods. Systematic Biology 47:228–253.

Wilcox, T. P., D. J. Zwickl, T. A. Heath, and D. M. Hillis. 2002. Phylogenetic relationships of the dwarf boas and a comparison of Bayesian and bootstrap measures of phylogenetic support. Molecular Phylogenetics and Evolution 25:361–371.

Wilgenbusch, J., and K. de Queiroz. 2000. Phylogenetic relationships among the phrynosomatid sand lizards inferred from mitochondrial DNA sequences generated by heterogeneous evolutionary processes. Systematic Biology 49:592–612.

Williams, E. E. 1969. The ecology of colonization as seen in the zoogeography of anoline lizards on small islands. The Quarterly Review of Biology 44:345–389.

———. 1972. The origin of faunas. Evolution of lizard congeners in a complex island fauna: a trial analysis. Pp. 47–89. *In* T. Dobzhansky, M. K. Hecht, and W. C. Steere (Eds.), Evolutionary Biology. Appleton-Century-Crofts, New York, New York, U.S.A.

———. 1976. West Indian anoles: a taxonomic and evolutionary summary 1. Introduction and a species list. Breviora 440:1–21.

———. 1983. Ecomorphs, faunas, island size, and diverse end points in island radiations of *Anolis*. Pp. 326–370. *In* R. B. Huey, E. R. Pianka, and T. W. Schoener (Eds.), Lizard Ecology. Harvard University Press, Cambridge, Massachusetts, U.S.A.

———. 1989. A critique of Guyer and Savage (1986): cladistic relationships among anoles (Sauria: Iguanidae): are the data available to reclassify the anoles? Pp. 434–478. *In* C. A. Woods (Ed.), Biogeography of the West Indies: Past, Present, and Future. Sandhill Crane Press, Gainesville, Florida, U.S.A.

Williams, E. E., H. Rand, A. S. Rand, and R. J. O'Hara. 1995. A computer approach to the comparison and identification of species in difficult taxonomic groups. Breviora 502:1–47.

Yang, Z. 1996. Phylogenetic analyses using parsimony and likelihood methods. Journal of Molecular Evolution 42:294–307.

Appendix I

Morphological Character Descriptions

For scale count characters that were variable on the right and left side of the same specimen, each side was scored separately. For meristic characters, ranges of raw counts are provided.

1. Head scales other than the supraoculars smooth to rugose (0); carinate to striate (1) (modified from Williams et al., 1995; Character 1). "Rugose" refers to numerous granular projections on the surface of the scales; "striate" refers to a ribbed texture of the scale surface. Williams et al. (1995) distinguished carinate and striate as separate states; however, taxa in this study have both carinate and striate scales, or delineation between the two states is not obvious.

2. Scales of the supraocular disk carinate (0); smooth (1) (this study). Williams et al. (1995) suggested scoring the head scale condition (character 1 in this study) on the supraocular disk. However, at least in the *cristatellus* series, variation between these two characters is not concordant and they are therefore treated separately.

3. Number of scales in contact with the rostral scale (Williams et al., 1995; Character 3). Range 3–9. This count includes both the postrostral and nasal scales but not the supralabials.

4. Number of canthal scales (this study). Range = 4–10. Counts were taken from the first canthal scale (included) to the rostral scale (excluded) along the canthal ridge, on both the right and left sides.

5. Minimum number of scales between the left and right second canthal scales (Williams et al., 1995; Character 2). Range = 4–12.

6. Minimum number of scales between the supraorbital semicircles (Williams et al., 1995; Character 6). Range = 0–4.

7. Minimum number of scales between interparietal scale and supraorbital semicircles (Williams et al., 1995; Character 13). Range = 0–9. Counts were taken separately for the right and left sides.

8. Superciliary scales posterior to elongate superciliaries large and rectangular (0); small and circular (1) (modified from Williams et al., 1995; Character 9). Williams et al. (1994) recognized three states, distinguishing between granular and small scales but acknowledging that the distinction was not clear cut. Therefore, we treated these two conditions as a single state.

9. Minimum number of loreal scales between the first canthal scale and the supralabial scales (modified from Williams et al., 1995; Character 10). Range = 3–10. Williams et al. (1995) coded the number of loreal scale rows as a character. The scale rows in question are sometimes incomplete, and counts of their precise number are frequently not repeatable among observers. Therefore, we used the minimum scale count between two reference points instead.

10. Minimum number of scales separating the subocular and supralabial scale rows (Williams et al., 1995; Character 15). Range = 0–1. Counts were taken separately for the right and left sides.

11. Minimum number of supralabial scales from the rostral scale to a point directly ventral to the center of the eye (Williams et al., 1995; Character 16). Range = 5–8. Counts were taken separately for the right and left sides.

12. Number of scales in contact with the mental scale (Williams et al., 1995; Character 17). Range = 4–10. This character was counted as the number of scales having any contact with the mental scale between, but not including, the infralabials.

13. Number of sublabial scales in contact with the infralabial scales (Williams et al., 1995; Character 19). Range = 0–5. Counts were taken separately for the right and left sides.

14. Dorsal scales small, round, raised, sometimes pointed or conical, non-imbricate, may be enlarged toward the midline of the body and may have granules between scales (0); large, flat, strongly keeled, imbricate (1) (modified from Williams et al., 1995; Characters 20 and 21).

15. Ventral belly scales smooth (0); carinate (1) (Williams et al., 1995; Character 25).

16. Toe pad on third (antepenultimate) phalanx of left hind foot (pes) extends distally to overlap second (penultimate) phalanx ventrally (0); does not overlap second (penultimate) phalanx (1) (Williams et al., 1995; Character 27). The extensions of lamellae-bearing toe pads are well-developed in all species in this study except *A. poncensis* and some *A. pulchellus*, in which they are extremely small (state 1).

17. Number of subdigital lamellae (Williams et al., 1995; Character 28). Range = 14–30. Counted on the toe pad of phalanges three and four (counting distal to proximal) of the fourth digit of the left hind foot (pes).

18. Supradigital scales multicarinate (0); smooth (1) (Williams et al., 1995; Character 29).

19. Tail crest absent, neural spines do not extend dorsally beyond the epaxial muscles (0); tail with middorsal crest, enlarged neural spines of the caudal vertebrae

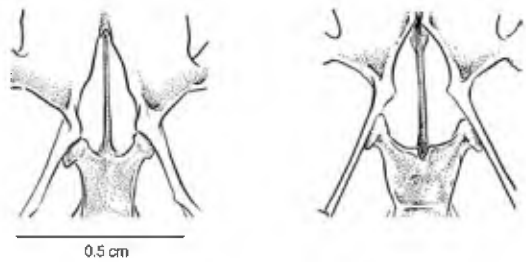

Fig. 10.—Character 23, state 0, *Anolis acutus* JBL 866 (left); state 1, *A. desechensis* USNM 221705 (right).

FIG. 11.—Character 24, state 0, *Anolis scriptus* USNM 81257 (left); state 1, *A. distichus ravitergum* USNM 259498 (right).

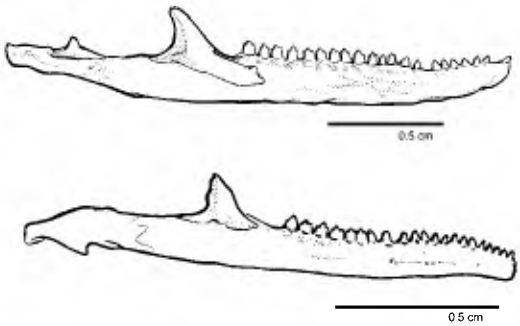

FIG. 12.—Character 29, state 0, *Anolis cristatellus* USNM 221693 (top); state 1, *A. distichus ravitergum* USNM 259498 (bottom).

extend dorsally beyond the epaxial muscles (1) (Williams et al., 1994; Character 31). Scored only in adult males. Williams et al. (1994) recognized "distinct crest" and "high crest" as separate character states. Because these conditions grade continuously into one another, we united them in a single state. In several species in which adult males develop a tail crest, some specimens identified as adult males lacked such a crest. We scored those species as having tail crests present at a frequency of 100% under the assumption that the specimens in question had not yet developed a crest (which occurs relatively late in ontogeny) rather than the alternative possibility that they would never have developed one (i.e., that variable presence of tail crests results from a genetic polymorphism).

20. Number of presacral vertebrae (Etheridge, 1959). Range 23–25.

21. Numbers of attached (i.e., to bony ribs) and free post-xiphisternal inscriptional ribs 3:1 (0); 2:2 (1); 1:3 (2) (Etheridge, 1959).

22. Parietal foramen located within the fronto-parietal suture (0); entirely within the parietal bone (1) (Etheridge, 1959). Because the area of the parietal that includes the parietal foramen remains unossified in juveniles (Etheridge, 1959), this character was scored only in adults. State 1 includes cases in which the foramen is located within the parietial but connected to the fronto-parietal suture by an orthogonal suture.

23. Basipterygoid processes of basisphenoid do not develop anteroventral crests so that the ventral surface of the basisphenoid forms a continuous surface from the corpus to the parasphenoid rostrum (0); basipterygoid processes develop bony crests that extend anteroventrally separating the corpus of the basisphenoid from the parasphenoid rostrum (when most highly developed, these crests contact one another medially below the base of the parasphenoid rostrum) (1) (this study; Fig. 10).

24. Postfrontal absent (0); barely extends or does not extend beyond the posterolateral process of the frontal that articulates with the postorbital (1); extends well beyond the posterolateral processes of the frontal, often expanding laterally over the medial surface of the postorbital (2); or posseses an intermediate state (3) (this study; Fig. 11).

25. Posteromedial crest of the parietal roof present (0); absent (1) (modified from Etheridge, 1959). Any development of a median parietal crest was coded 0. Actual lengths of the parietal crest ranged from 0.5–5.0 mm in the specimens examined in this study. This character has traditionally been described as the shape of the crests bounding the parietal roof, with the states coded as trapezoidal, V-shaped, or Y-shaped, (Etheridge, 1959; see illustrations in Etheridge, 1959; Cannatella and de

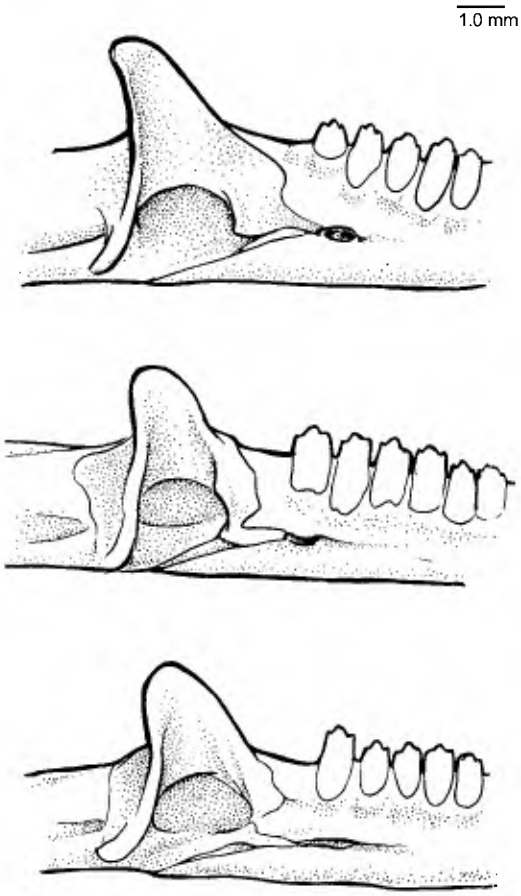

FIG. 13.—Character 30, state 0, and character 31, state 1, *Anolis gingivinus* USNM 315638 (top); character 30, state 1, and character 31, state 0, *A. desechensis* USNM 221701 (middle); character 30, state 2, *A. gundlachi* USNM 221729 (bottom).

Queiroz, 1989; Poe 1998). However, the V-shaped condition is merely the transition point, when the lateral crests bounding the parietal roof first meet posteromedially, between the trapezoidal condition (no contact between lateral crests) and the Y-shaped condition (lateral crests contact to form a posteromedial crest). Moreover, those lizards that develop a Y-shaped roof (i.e., a posteromedial crest) pass through trapezoidal and V-shaped stages ontogenetically. For these reasons, we recognized only two states (absence or presence of the posteromedial crest) and scored the character only in adult specimens.

26. Number of premaxillary teeth (de Queiroz, 1987). Range = 8–14.

27. Sculpturing on ventrolateral surface of the dentary *cybotes* type: a single, deep semilunar groove (0); absent (1); *cristatellus* type: irregular, longitudinal ridges and grooves (2); *krugi* type: deep semilunar ridges and grooves (3) (Etheridge, 1959: Fig. 8). When present, dentary sculpturing occurs only in adult males (Etheridge, 1959), and therefore we scored this character only for such specimens. Etheridge (1959) reported sculpturing to be absent in *A. poncensis*; however, all adult male *A. poncensis* examined in this study possess dentary sculpturing.

28. Splenial absent (0); present (1) (Etheridge, 1959).

29. Lateral process of the coronoid extended anteriorly, projects well beyond the part of the jaw directly ventral to the coronoid process (0); truncated anteriorly, mostly confined to the part of the jaw ventral to the coronoid process (1) (this study; Fig. 12).

30. Dentary lacks a distinct posterior process on the lingual surface of the jaw that overlaps the coronoid posterodorsal to the anterior alveolar mylohyoid foramen so that the coronoid forms the posterior margin of the foramen (0); posterior process of the dentary overlaps the coronoid posterodorsal to the anterior alveolar/mylohyoid foramen but does not contact the ventral part of the dentary posterior to the foramen so that the coronoid forms the posterior margin of the foramen (1); posterior process of the dentary overlaps the coronoid and contacts the ventral part of the dentary so that the coronoid is excluded from the margin of the anterior alveolar/mylohyoid foramen, which is surrounded entirely by the dentary (2) (this study; Fig. 13). The single foramen near the junction of the dentary, splenial, and coronoid bones on the lingual surface of the lower jaw in anoles is assumed to correspond with both the anterior inferior alveolar foramen and the anterior mylohyoid foramen of other iguanids (e.g., Oelrich, 1958), though we have not verified that both the inferior alveolar nerve and the anterior mylohyoid nerve pass through it.

31. Anterior end of the splenial abuts with or only slightly overlaps the coronoid posterior to the anterior alveolar/mylohyoid foramen (0); extensively overlaps the coronoid, often contacting the anterior alveolar/mylohyoid foramen or the part of the dentary that extends posterodorsal to the foramen (1) (this study; Fig. 13). Taxa lacking a splenial (character 26) were not scored for this character.

32. Diploid chromosome complement of females (2n) = 36 (0); 2n = 34 (1); 2n = 32 (2); 2n = 30 (3); 2n = 28 (4); 2n = 26 (5). Linear order in MANOB analyses.

33. No obvious sex chromosome heteromorphism (0); X_1X_2Y male sex chromosome heteromorphism with Y chromosome metacentric (1); XY male sex chromosome heteromorphism with Y chromosome acrocentric (2). Linear order in MANOB analyses.

Appendix II

Morphological Data Set

Cell entries are character states and (parenthetically) their frequencies, when these are less than 1.00, as well as Sample sizes (N). "?" indicates that the character could not be scored for that taxon.

Character		*acutus*	*brevirostris*	*cooki*	*cristatellus*	*cybotes*	*desechensis*	*distichus*	*ernest-williamsi*	*evermanni*	*gingivinus*	*gundlachi*	*krugi*	*monensis*	*poncensis*	*pulchellus*	*scriptus*	*stratulus*	*wattsi*
1		0	0	0	0	0	0	0	0	0	0	1	1	1	1	0 (.17) 1 (.83)	0	0 (.96) 1 (.04)	0
	N =	10	13	10	45	17	23	15	10	8	8	22	22	16	2	24	10	25	10
2		0 (.60) 1 (.40)	1	0 (.90) 1 (.10)	0 (.91) 1 (.09)	0 (.94) 1 (.06)	0	0 (.33) 1 (.67)	0	0 (.87) 1 (.13)	0 (.30) 1 (.70)	0	0	0 (.94) 1 (.06)	0	0	0	0 (.92) 1 (.08)	1
	N =	10	13	10	44	17	23	15	6	9	10	22	21	16	2	25	10	24	10
3		5 (.70) 6 (.20) 7 (.10)	4 (.77) 5 (.15) 6 (.08)	5	5 (.55) 6 (.31) 7 (.12) 9 (.02)	5 (.18) 6 (.53) 7 (.24) 9 (.05)	5 (.96) 6 (.04)	4 (.07) 5 (.13) 6 (.60) 7 (.20)	5 (.30) 6 (.50) 7 (.20)	4 (.20) 5 (.80)	5	7 (.92) 8 (.04) 9 (.04)	5 (.92) 6 (.08)	5 (.75) 6 (.19) 7 (.06)	4	3 (.04) 4 (.29) 5 (.61) 6 (.07)	5 (.90) 6 (.10)	5 (.64) 6 (.12) 7 (.20) 8 (.04)	5 (.70) 6 (.30)
	N =	10	13	10	51	17	23	15	10	10	10	25	25	16	8	28	10	25	10
4		5 (.10) 6 (.35) 7 (.50) 8 .05)	5 (.35) 6 (.58) 7 (.08)	5 (.10) 6 (.65) 7 (.25)	5 (.13) 6 (.58) 7 (.29) 8 (.01)	5 (.12) 6 (.41) 7 (.38) 8 (.09)	5 (.07) 6 (.70) 7 (.22) 8 (.02)	4 (.07) 5 (.40) 6 (.53)	6 (.05) 7 (.65) 8 (.30)	6 (.20) 7 (.45) 8 (.30) 9 (.05)	6 (.40) 7 (.60)	6 (.04) 7 (.42) 8 (.50) 9 (.04)	5 (.24) 6 (.62) 7 (.12) 8 (.02)	6 (.38) 7 (.56) 8 (.06)	5 (.69) 6 (.25) 7 (.06)	4 (.04) 5 (.16) 6 (.63) 7 (.14) 8 (.04)	6 (.50) 7 (.50)	6 (.10) 7 (.38) 8 (.40) 9 (.10)	5 (.05) 6 (.95)
	N =	10	13	10	52	17	23	15	10	10	10	25	25	16	8	28	10	25	10
5		5 (.20) 6 (.70) 8 (.10)	4 (.69) 5 (.08) 6 (.15) 8 (.08)	5 (.50) 6 (.30) 7 (.20)	4 (.27) 5 (.40) 6 (.21) 7 (.08) 8 (.04)	5 (.18) 6 (.41) 7 (.35) 8 (.06)	4 (.09) 5 (.61) 6 (.26) 7 (.04)	4 (.80) 5 (.20)	5 (.20) 6 (.50) 7 (.30)	5 (.50) 6 (.30) 7 (.10) 8 .10)	4 (.30) 5 (.70)	8 (.20) 9 (.24) 10 (.24) 11 (.28) 12 (.04)	4 (.08) 5 (.20) 6 (.52) 7 (.20)	4 (.13) 5 (.25) 6 (.31) 7 (.19) 8 (.06) 9 (.06)	4 (.35) 5 (.50) 6 (.25)	4 (.18) 5 (.25) 6 (.36) 7 (.18) 8 (.04)	5 (.10) 6 (.60) 7 (.30)	4 (.04) 5 (.20) 6 (.20) 7 (.36) 8 (.20)	5 (.50) 6 (.40) 7 (.10)
	N =	10	13	10	52	17	23	15	10	10	10	25	25	16	8	28	10	25	10
6		0	0	0	0	0 (.59) 1 (.41)	0	0 (.93) 1 (.07)	0	0 .50) 1 (.50)	0 (.80) 1 (.20)	1 (.08) 2 (.44) 3 (.44) 4 (.04)	0 (.04) 1 (.88) 2 (.08)	0	0 (.50) 1 (.50)	0 (.29) 1 (.68) 2 (.04)	0 (.90) 1 (.10)	0 (.67) 1 (.33)	0 (.60) 1 (.40)
	N =	10	13	10	52	17	23	15	10	10	10	25	25	16	8	28	10	24	10
7		0 (.40) 1 (.40) 2 (.20)	0 (.58) 1 (.42)	1 (.20) 2 (.60) 3 (.20)	1 (.09) 2 (.56) 3 (.25) 4 (.10)	1 (.29) 2 (.41) 3 (.24) 4 (.06)	1 (.02) 2 (.15) 3 (.52) 4 (.26)	0 (.43) 1 (.50) 2 (.07)	1 (.35) 2 (.60) 3 (.05)	1 (.25) 2 (.30) 3 (.35) 4 (.10)	1 (.30) 2 (.50) 3 (.20)	4 (.10) 5 (.32) 6 (.44) 7 (.08)	1 (.06) 2 (.50) 3 (.40) 4 (.04)	0 (.06) 1 (.50) 2 (.38) 3 (.06)	1 (.38) 2 (.50) 3 (.13)	1 (.05) 2 (.41) 3 (.43) 4 (.07)	2 (.45) 3 (.45) 4 (.10)	1 (.32) 2 (.58) 3 (.10)	1 (.10) 2 (.25) 3 (.55) 4 (.10)

Appendix II

Continued.

Character		*acutus*	*brevirostris*	*cooki*	*cristatellus*	*cybotes*	*desechensis*	*distichus*	*ernest-williamsi*	*evermanni*	*gingivinus*	*gundlachi*	*krugi*	*monensis*	*poncensis*	*pulchellus*	*scriptus*	*stratulus*	*wattsi*
					5 (.01)		5 (.04)					8 (.02) 9 (.04)				5 (.02) 6 (.02)			
	N =	10	13	10	52	17	23	15	10	10	10	25	25	16	8	28	10	25	10
8		0	1	0	0	0	0	1	0	1	0	0	0	0	0	0	0	1	0
	N =	10	13	10	52	17	23	15	10	10	10	25	25	16	8	28	10	25	10
9		4 (.20) 5 (.75) 6 (.05)	4 (.50) 5 (.38) 6 (.12)	5 (.75) 6 (.25)	4 (.02) 5 (.31) 6 (.42) 7 (.22) 8 (.03)	5 (.03) 6 (.47) 7 (.38) 9 (.09) 10 (.03)	5 (.26) 6 (.72) 7 (.02)	4 (.47) 5 (.47) 6 (.07)	6 (.60) 7 (.40)	4 (.10) 5 (.70) 6 (.20)	4 (.60) 5 (.20) 6 (.20)	6 (.22) 7 (.46) 8 (.28) 9 (.04)	4 (.04) 5 (.42) 6 (.50) 7 (.04)	4 (.19) 5 (.50) 6 (.31)	3 (.06) 4 (.94)	3 (.07) 4 (.38) 5 (.50) 6 (.05)	4 (.20) 5 (.60) 6 (.20)	4 (.32) 5 (.56) 6 (.12)	5 (.90) 6 (.10)
	N =	10	13	10	52	17	23	15	10	10	10	25	25	16	8	28	10	25	10
10		0	0	0	0 (.77) 1 (.23)	0 (.06) 1 (.91) 2 (.03)	0 (.89) 1 (.11)	0	0	0	0	0	0	0	0	0	0	0	0
	N =	10	13	10	52	17	23	15	10	10	10	25	25	16	8	28	10	25	10
11		6 (.70) 7 (.30)	5 (.19) 6 (.77) 7 (.04)	6 (.45) 7 (.55)	5 (.01) 6 (.56) 7 (.42) 8 (.01)	6 (.21) 7 (.71) 8 (.08)	5 (.02) 6 (.30) 7 (.63) 8 (.04)	5 (.30) 6 (.60) 7 (.10)	6 (.50) 7 (.50)	6 (.55) 7 (.35) 8 (.10)	6 (.20) 7 (.70) 8 (.10)	6 (.42) 7 (.48) 8 (.10)	5 (.04) 6 (.50) 7 (.44) 8 (.02)	6 (.19) 7 (.69) 8 (.13)	5 (.06) 6 (.81) 7 (.13)	5 (.13) 6 (.67) 7 (.20)	5 (.15) 6 (.85)	5 (.06) 6 (.34) 7 (.50) 8 (.10)	6 (.85) 7 (.15)
	N =	10	13	10	52	17	23	15	10	10	10	25	25	16	8	28	10	25	10
12		4 (.10) 5 (.20) 6 (.50) 7 (.20)	6 (.46) 7 (.23) 8 (.31)	6 (.30) 7 (.30) 8 (.30) 9 (.10)	6 (.25) 7 (.24) 8 (.47) 9 (.04)	6 (.82) 7 (.12) 8 (.06)	6 (.13) 7 (.09) 8 (.65) 9 (.09) 10 (.04)	6 (.20) 7 (.20) 8 (.13) 9 (.27) 10 (.20)	5 (.11) 6 (.44) 7 (.11) 8 (.33)	6 (.30) 7 (.10) 8 (.40) 9 (.20)	6 (.50) 7 (.20) 8 (.30)	4 (.04) 6 (.28) 7 (.28) 8 (.24) 9 (.16)	4 (.04) 5 (.08) 6 (.80) 7 (.04) 8 (.04)	5 (.06) 6 (.56) 7 (.31) 8 (.06)	4 (.25) 5 (.50) 6 (.25)	4 (.14) 5 (.14) 6 (.64) 7 (.04) 8 (.04)	6 (.10) 7 (.30) 8 (.30) 9 (.20) 10 (.10)	6 (.08) 7 (.16) 8 (.44) 9 (.28) 10 (.04)	6 (.60) 7 (.10) 8 (.10) 9 (.10) 10 (.10)
	N =	10	13	10	51	17	23	15	9	10	10	25	25	16	8	28	10	25	10
13		1 (.25) 2 (.75)	2 (.08) 3 (.81) 4 (.08) 5 (.04)	1 (.40) 2 (.60)	0 (.02) 1 (.71) 2 (.24) 3 (.03)	1 (.09) 2 (.65) 3 (.26)	1 (.59) 2 (.41)	2 (.13) 3 (.80) 4 (.07)	1 (.30) 2 (.70)	1 (.65) 2 (.35)	1 (.05) 2 (.80) 3 (.10) 4 (.05)	1 (.80) 2 (.20)	1 (.72) 2 (.26) 3 (.02)	1 (.06) 2 (.91) 3 (.03)	1	1 (.79) 2 (.21)	1 (.15) 2 (.75) 3 (.10)	1 (.10) 2 (.72) 3 (.16) 4 (.02)	1 (.95) 2 (.05)
	N =	10	13	10	52	17	23	15	10	10	10	25	25	16	8	28	10	25	10
14		0	0	0	0	0	0	0	0	0	0	0	0	0	1	0	0	0	0
	N =	10	13	8	43	17	19	15	10	8	8	24	20	13	2	23	10	25	10

Appendix II

Continued.

Character		*acutus*	*brevirostris*	*cooki*	*cristatellus*	*cybotes*	*desechensis*	*distichus*	*ernest-williamsi*	*evermanni*	*gingivinus*	*gundlachi*	*krugi*	*monensis*	*poncensis*	*pulchellus*	*scriptus*	*stratulus*	*wattsi*
15		1	0	1	0 (.50) 1 (.50)	0	0 (.35) 1 (.65)	0	0	0	0	1	1	0 (.87) 1 (.13)	1	1	0 (.70) 1 (.30)	0	1
	N =	10	13	10	52	17	23	15	4	10	10	25	25	16	8	28	10	25	10
16		0	0	0	0	0	0	0	0	0	0	0	0	0	1	0 (.66) 1 (.33)	0	0	0
	N =	10	13	5	44	17	19	15	10	8	8	23	18	13	5	21	10	25	10
17		22 (.20) 23 (.30) 24 (.20) 25 (.20) 26 (.10)	16 (.39) 17 (.23) 18 (.08) 19 (.15) 20 (.15)	20 (.14) 21 (.29) 22 (.57)	20 (.02) 21 (.22) 22 (.22) 23 (.35) 24 (.08) 25 (.08) 26 (.02)	15 (.05) 17 (.18) 18 (.24) 19 (.24) 20 (.24) 21 (.05)	20 (.04) 21 (.04) 22 (.13) 23 (.09) 24 (.04) 25 (.13) 26 (.26) 27 (.22) 28 (.04)	17 (.13) 18 (.20) 19 (.13) 20 (.20) 21 (.27) 23 (.07)	20 (.10) 21 (.20) 22 (.10) 23 (.10) 24 (.20) 25 (.30)	26 (.10) 27 (.10) 28 (.40) 29 (.20) 30 (.20)	20 (.10) 21 (.40) 22 (.20) 23 (.30)	16 (.08) 18 (.17) 19 (.33) 20 (.25) 21 (.13) 22 (.04)	18 (.04) 19 (.08) 20 (.08) 21 (.28) 22 (.32) 23 (.16) 24 (.04)	17 (.06) 19 (.06) 20 (.13) 21 (.25) 22 (.25) 23 (.19) 24 (.06)	14 (.17) 15 (.17) 16 (.33) 18 (.17) 19 (.17)	18 (.04) 19 (.11) 20 (.22) 21 (.26) 22 (.26) 23 (.07) 24 (.04)	22 (.40) 23 (.20) 24 (.10) 25 (.20) 27 (.10)	20 (.08) 21 (.36) 22 (.16) 23 (.28) 24 (.08) 26 (.04)	18 (.30) 19 (.60) 20 (.10)
	N =	10	13	10	49	17	23	15	10	10	10	24	25	16	6	27	10	25	10
18		0	1	0	0	0	0	0	0	0	0	0	0	0	0	0	0	1	0
	N =	10	13	10	52	17	23	15	10	10	10	25	25	16	8	28	10	25	10
19		1	0	1	1	0	1	0	1	0	0	1	0	1	0	0	1	0	0
	N =	4	5	1	18	14	14	3	1	3	2	10	16	7	2	20	3	18	4
20		23 (.08) 24 (.92)	24	23	23	23 (.04) 24 (.96)	23	24 (.97) 25 (.03)	23	24	24	23	23	23 (.93) 24 (.07)	23	23	23	24	24
	N =	13	17	9	27	28	10	30	6	17	14	16	18	17	19	17	27	21	5
21		0	0 (.93) 1 (.07)	1	0 (.04) 1 (.96)	0	1	0	1	0	0	1	1	0 (.07) 1 (.93)	1	1 (.88) 2 (.12)	0 (.05) 1 (.95)	0	0 (.80) 1 (.20)
	N =	10	14	7	25	22	10	28	6	11	10	10	14	14	14	16	19	19	5
22		0	0	1	1	0	1	0	1	0 (.67) 1 (.33)	0 (.78) 1 (.22)	1	0 (.80) 1 (.20)	0 (.43) 1 (.57)	0 (.20) 1 (.80)	0 (.80) 1 (.20)	0 (.30) 1 (.70)	0	0 (.70) 1 (.30)
	N =	5	9	3	9	13	22	12	1	9	9	7	10	7	5	10	10	6	10
23		0	0	1	1	0	1	0	1	0	0	0 (.14) 1 (.86)	0 (.11) 1 (.89)	1	0	0	1	0	0
	N =	5	9	3	9	13	22	12	1	9	9	7	9	9	5	10	9	6	10
24		1	3	1	1	0 (.92)	1	3	?	2	1	1 (.89)	0 (.11)	1	1	1	1	2	1

Appendix II

Continued.

Character		*acutus*	*brevirostris*	*cooki*	*cristatellus*	*cybotes*	*desechensis*	*distichus*	*ernest-williamsi*	*evermanni*	*gingivinus*	*gundlachi*	*krugi*	*monensis*	*poncensis*	*pulchellus*	*scriptus*	*stratulus*	*wattsi*
						3 (.08)						2 (.11)	1 (.89)						
	N =	4	10	10	13	13	23	19		9	15	9	9	6	5	10	9	4	10
25		0 (.80)	0 (.10)	0	0	0	0	0 (.58)	0	1	0 (.89)	0	0 (.90)	0	0 (.80)	0	0	1	0
		1 (.20)	1 (.90)					1 (.42)			1 (.11)		1 (.10)		1 (.20)				
	N =	5	10	3	8	4	22	12	1	9	9	7	10	7	5	10	9	6	9
26		9 (.17)	9 (.25)	9 (.10)	8 (.09)	9 (.11)	10 (.14)	8 (.16)	14	10 (.13)	10 (.07)	9 (.56)	11 (.22)	10 (.33)	8 (.20)	10 (.10)	11 (.50)	9 (.20)	10 (.20)
		10 (.17)	10 (.25)	10 (.50)	9 (.09)	10 (.27)	11 (.59)	9 (.16)		11 (.25)	11 (.21)	10 (.22)	12 (.11)	11 (.50)	9 (.60)	11 (.10)	12 (.20)	11 (.20)	11 (.30)
		11 (.50)	11 (.38)	11 (.30)	10 (.18)	11 (.28)	12 (.18)	10 (.58)		12 (.13)	12 (.57)	13 (.22)	13 (.56)	12 (.17)	10 (.20)	12 (.70)	13 (.30)	13 (.40)	12 (.30)
		13 (.17)	13 (.13)	12 (.10)	11 (.27)	12 (.27)	13 (.09)	11 (.11)		13 (.38)	13 (.07)		14 (.11)			13 (.10)			13 (.20)
					13 (.36)	13 (.11)				14 (.12)	14 (.07)								
	N =	6	8	10	11	11	22	19	1	8	14	9	9	6	5	10	10	5	10
27		1	1	2	2	0	2	1	2	1	1	3	3	2 (.14)	1 (.20)	2 (.11)	2	1	1
														3 (.86)	2 (.80)	3 (.89)			
	N =	1	7	3	7	9	12	4	1	2	6	2	4	9	6	9	6	6	10
28		1 (.67)	1	1	1	0	1	1	1	0	0 (.07)	1	0 (.10)	1	0	0 (.11)	1	0	1 (.50)
		0 (.33)									1 (.93)		1 (.90)			1 (.89)			0 (.50)
	N =	6	11	10	14	13	23	15	1	9	15	9	10	7	5	9	10	6	10
29		0	1	0	0	0	0	1	0	0	0	0	0	0	0	0	0	0	0
	N =	5	11	3	9	13	21	12	1	9	9	7	9	9	5	9	9	6	10
30		0 (.17)	0 (.18)	0 (.10)	1 (.23)	0 (.81)	0 (.04)	1 (.84)	1	1 (.44)	0	1 (.33)	0 (.10)	1 (.86)	2	1 (.56)	1	1 (.67)	0
		1 (.50)	1 (.73)	1 (.30)	2 (.77)	1 (.12)	1 (.96)	2 (.16)		2 (.56)		2 (.67)	1 (.40)	2 (.14)		2 (.44)		2 (.33)	
		2 (.33)	2 (.09)	2 (.60)		2 (.07)							2 (.50)						
	N =	6	11	10	13	13	23	19	1	9	15	9	10	7	5	9	10	6	10
31		1	0 (.91)	0 (.13)	0 (.17)	?	0 (.22)	0	1	?	0 (.93)	0 (.33)	0 (.29)	0 (.33)	?	0 (.50)	0 (.56)	?	?
			1 (.09)	1 (.87)	1 (.83)		1 (.78)				1 (.07)	1 (.67)	1 (.71)	1 (.67)		1 (.50)	1 (.44)		
	N =	4	11	8	6		23	19	1		14	3	7	6		6	9		
32		2	?	3	4	0	?	1	?	5	3	3	3	3	3	3	4	3	3
33		1	?	1	1	0	?	1	?	2	1	1	1	1	1	1	1	1	1

Appendix III

Fluid-Preserved Specimens Examined

Museum abbreviations follow Leviton et al. (1985). All specimens are USNM unless otherwise indicated. REG, JBL, LGP, and KdQ refer to the field catalogs of Richard E. Glor, Jonathan B. Losos, Linnette García-Pérez, and Kevin de Queiroz, respectively. RE refers to radiograph data collected by Richard Etheridge for his 1959 dissertation.

Anolis acutus—VIRGIN ISLANDS: St. Croix: 12215, 78929–36, 539330–2, UMMZ lot 73677 (5 specimens; RE). *Anolis brevirostris*—DOMINICAN REPUBLIC: Barahona: 329016–7, 329019, 329021–5; Pedernales: 286874, 314295–6, 328539; HAITI: Ouest: 329026. *Anolis brevirostris wetmorei*—DOMINICAN REPUBLIC: Barahona: 260253–8. *Anolis cooki*—PUERTO RICO: Guánica: 286821, 304659, 321858–63, 327071–2. *Anolis cristatellus cristatellus*—DOMINICAN REPUBLIC: La Romana: 314323–4; PUERTO RICO: Arecibo: 165797; Arroyo: 25587, 25589; Caguas: 25671, 25678; Cayey: 25526; Ciales: 209671; Dorado: 209669–70; Guánica: 86555, 304658; Humacao: 27772; Lajas: 327098; Lares: 25543; Magueyes: 127880, 221132–3; Manatí: 86527; Maricao: 209667; Ponce: 327083, 327088; Río Piedras: 286823; Utuado: 304653; Yauco: 209665. *Anolis cristatellus wileyae*—BRITISH VIRGIN ISLANDS: Anegada: 140309–10; PUERTO RICO: Isla de Culebra: 26093, 26097, UMMZ lot 73648 (2 specimens; RE); Isla de Vieques: 221410, 221424, 221458–9; VIRGIN ISLANDS: Beef Island: 221470, 314229; Guana Island: 314233; Jost Van Dyke: 304579; Norman Island: 304573; St. John: 304602, lot 196310 (2 specimens); St. Thomas: 98948, 304613, 304620; Tortola: 221597, 221608, 221615, 221645; Virgin Gorda: 304595, 304597; Water Island: 115879. *Anolis cybotes*—DOMINICAN REPUBLIC: Barahona: 286877–81; Isla Catalina: 260349, 260351, 220909–14, 220916; La Vega: 259393–4; Samana: 260383–5, 260393, 260395–6; HAITI: UMMZ lot 92909 (3 specimens; RE); Île de la Gonâve: 77072, 239384; Nord: 239378–9. *Anolis desechensis*—PUERTO RICO: Isla Desecheo: 220942–4, 220946–7, 220949, 220952–3, 220956, 220959–60, 220963–4, 22096–68, 220973, 220981, 220989–91, 220993–4. *Anolis distichus biminensis*—BAHAMAS: Bimini Island: AMNH 68638 (RE), AMNH lot 68639 (5 specimens; RE). *Anolis distichus distichoides*—BAHAMAS: Andros Island: 56938, UMMZ lot 115597 (6 specimens; RE); Eleuthra Island: UMMZ lot 115588 (4 specimens; RE). *Anolis distichus dominicensis*—DOMINICAN REPUBLIC: Monte Cristi: 224959; HAITI: Nord: 239388. *Anolis distichus favillarum*—DOMINICAN REPUBLIC: Barahona: 259403–4, 259408. *Anolis distichus ignigularis*—DOMINICAN REPUBLIC: El Seibo: 260448, 260450–2. *Anolis distichus patruelis*—HAITI: Petit Cayemites: 80815, 80817. *Anolis distichus properus*—DOMINICAN REPUBLIC: La Altagracia: Boca de Yuma: 259413–4. *Anolis distichus ravitergum*—DOMINICAN REPUBLIC: Azua: Azua: 259400; Azua: Peralta: 224960. *Anolis distichus sejunctus*—DOMINICAN REPUBLIC: Isla Saona: 260509. *Anolis ernestwilliamsi*—BRITISH VIRGIN ISLANDS: Carrot Rock: MCZ 158398, MCZ 159400–4, UMMZ 200151–4. *Anolis evermanni*—PUERTO RICO: Catalina Plantation NE side of El Yunque Mtn.: 26853, 26855, 26861, 26866; El Verde: 304652; El Yunque: 221149, 327112–14; Lares: 304655; Maricao: 209673–4, 304651. *Anolis gingivinus*—ANGUILLA: 236268, 236273–4, 236277, 336538–9; ST. BARTHELEMY: 236308, 236310–1; ST. Martin: 315535–7, 31552-3. *Anolis gundlachi*—PUERTO RICO: Adjuntas: 25600, 27246–49, 27262, 27268, 58859–60; El Yunque: 26805, 26901, 26903, 221150–2, 327119–25; Maricao: 209675–6; Yabucoa: 221148, 327116. *Anolis krugi*—PUERTO RICO: Adjuntas: 25597–8, 27277; Catalina Plantation between Mameyes and Luquillo: 26874, 26898, 26993; El Yunque: 327129; Juana Díaz: 221154–6; Lares: 25460; Magueyes: 304650, 336301; Maricao: 209677; Palmer: 221158, 221164–6, 327132; Utuado: 25512, 27157, 27159, 27161, 27200, 58366, 304660, Yabucoa: 221157. *Anolis monensis*—PUERTO RICO: Isla Mona: UMMZ lot 73694 (2 specimens; RE), 133681–2, lot 196582 (2 specimens), 212287–91, 229880, 304661–4, 532430; Isla Monita: 229893–4. *Anolis poncensis*—PUERTO RICO: Guánica: 304657; Lajas: 286831, 327137; Ponce: 27289–94. *Anolis pulchellus*—BAHAMAS: Nassau: 25651 (locality questionable); PUERTO RICO: Aguadilla: 212315; Añasco: 25483, 25486; Arecibo: 86542, 86545; Ciales: 209679; Coamo: 212317; Dorado: 209678; Juana Díaz: 212316, 221176; Lajas: 327136; Magueyes-Lajas: 221167, 221171; Isla Palominas: 90351; Ponce: 27282, 27284, 27286; San Juan: 26809, 26813; Utuado: 27199; Isla de Vieques: 221435; 221439; VIRGIN ISLANDS: Jost Van Dyke: 304634; Norman Island: 304653; Tortola: 221619, 221647. *Anolis scriptus leucophaeus*—BAHAMAS: Great Inagua Island: 81252, 81254–5, 81257–8, 81262–4, 81266, 81268, UMMZ lot 115594 (6 specimens; RE). *Anolis scriptus mariguanae*—BAHAMAS: Mariguana: UMMZ 188060 (RE). *Anolis scriptus scriptus*—BAHAMAS: South Caicos Islands: 81415, 81419, 81420, 81425, UMMZ 115591 (RE), lot 115592 (3 specimens; RE), UMMZ 115593 (RE); Turk Islands: Long Cay: 81269, 81287–9. *Anolis stratulus*—PUERTO RICO: Adjuntes: 25457; Arroyo: 25533; Cayey: 25523; Dorado: 209680; El Yunque: 26849–50, 26992; Juana Díaz: 212319; San Juan: 127879; Utuado: 27163, 27193–4, 27196; Isla de Vieques: 27069–74, 221143–5; Yabucoa: 221177; VIRGIN ISLANDS: Anegada: 304637–8; Beef Island: 314236–8; St. John: 196309; St. Thomas: 98956, 304643; Tortola: 221627, 221648. *Anolis wattsi wattsi*—ANTIGUA: 19854–6, 218462–3, 218465, 218468–70, 509081.

Appendix IV

Osteological Specimens Examined

Anolis acutus—VIRGIN ISLANDS: St. Croix: MCZ 131552–6. *Anolis brevirostris*—DOMINICAN REPUBLIC: Barahona: 259476–81; Peravia: MCZ 152460, MCZ 152465, MCZ 152467; HAITI: Ouest: 521307–8. *Anolis cooki*—PUERTO RICO: Guánica: MCZ 93130, 321859; Playa Cana Gorda: MCZ 101895–8, MCZ 101907, MCZ 101911, MCZ 101913; Salinas: MCZ 61594. *Anolis cristatellus cristatellus*—DOMINICAN REPUBLIC: La Romana: 221829; PUERTO RICO: Coamo: 213674; El Verde: KdQ 1549–50; Magueyes: 221692, 221694; Pastillo: 226398; San Germán: LGP 0001, LGP 0003; Santa Rita: 221693. *Anolis cristatellus wileyae*—PUERTO RICO: Isla de Vieques: 221697; VIRGIN ISLANDS: St. John: CAS 166514, CAS 166516. *Anolis cybotes*—DOMINICAN REPUBLIC: UMMZ 1473–4, UMMZ 1476; Barahona:

259490–1, 259494; La Altagracia: 225039, 259487–8; HAITI: Sud: MCZ 134019, MCZ 134021, MCZ 134023, MCZ 134025. *Anolis desechensis*—PUERTO RICO: Isla Desecheo: 221698–706, 221709–21, 221723. *Anolis distichus dominicensis*—DOMINICAN REPUBLIC: Samana: 55060; HAITI: Les Cayes: 22568. *Anolis distichus favillarum*—DOMINICAN REPUBLIC: Barahona: 259499, 259503–4, 259507–8. *Anolis distichus ocior*—BAHAMAS: San Salvador Island: 220555–220557. *Anolis distichus properus*—DOMINICAN REPUBLIC: La Altagracia: 225043; San Pedro: 259495–6. *Anolis distichus ravitergum*—DOMINICAN REPUBLIC: Azua: 225040, 259498; Peravia: 225041–2. *Anolis ernestwilliamsi*—BRITISH VIRGIN ISLANDS: Carrot Rock: MCZ 165248. *Anolis evermanni*—PUERTO RICO: El Yunque: 327112, MCZ 119663, MCZ 119701–2, MCZ 142506; Maricao: MCZ 61809, 61813; North Loop: MCZ 119700; Palmer: MCZ 129785. *Anolis gingivinus*—ANGUILLA: 236356–8, 236360–4, 235368. ST. BARTHELEMY: 236366–7; ST. MARTIN: 315638, 315640–1, 315737. *Anolis gundlachi*—PUERTO RICO: El Verde Field Station: MCZ 132058 , 132062–3, 132069, 132504; El Yunque: MCZ 131917; Maricao: MCZ 61851; Palmer: 221729–30. *Anolis krugi*—El Verde Field Station: MCZ 132074, MCZ 132084–5, MCZ 132087, MCZ 132090; El Yunque: MCZ 131911; Mayagüez: MCZ 61909, MCZ 61916, MCZ 61919. *Anolis monensis*—PUERTO RICO: Isla Mona: MCZ 35636, MCZ 35638, MCZ 35648, MCZ 35673, MCZ 35693, 222805–6. *Anolis poncensis*—PUERTO RICO: Lajas: 327137; Punta Jaguey: MCZ 158234, 158236. *Anolis pulchellus*—PUERTO RICO: MCZ 131956, MCZ 131959, MCZ131963, MCZ 131967; Magueyes: 221734; Río Grande, 1.25 miles East: MCZ 131969; Isla de Vieques: 221733, 221735–7. *Anolis scriptus scriptus*—BAHAMAS: South Caicos Islands: MCZ 42070–2. *Anolis scriptus leucophaeus*—BAHAMAS: Great Inagua Island: 81257, MCZ 100505–6, MCZ 100508–9, MCZ 36773, MCZ 36779. *Anolis stratulus*—PUERTO RICO: San Germán: LGP 0004; UPR Campus: MCZ 131978, MCZ 131985; VIRGIN ISLANDS: St. Thomas: MCZ 131980, 131982. *Anolis wattsi wattsi*—ANTIGUA: St. John's Parish: 218332–8, 218342; St. Mary's Parish: 218344, 218346.

Appendix V

Localities and Voucher Specimens for Tissue Samples

For species with more than one specimen, the first listed was used in the final phylogenetic analyses.

Anolis acutus—VIRGIN ISLANDS: St. Croix: SW of Christiansted: Sugar Beach Condominium: JBL 869. *Anolis brevirostris*—DOMINICAN REPUBLIC: Pedernales: 17 km NW Oviedo: 314295. *Anolis cooki* 1—PUERTO RICO: Mayagüez: Bosque Estatal de Guánica: 321859. *Anolis cooki* 2—PUERTO RICO: Mayagüez: Bosque Estatal de Guánica: 321860. *Anolis cristatellus*—PUERTO RICO: Arecibo: Reserva Forestal Cambalache: 321867. *Anolis cybotes*—DOMINICAN REPUBLIC: Distrito Nacional: Peravia: El Recodo: KdQ 2105. *Anolis desechensis* 1—PUERTO RICO: Isla Desecheo: KdQ 1886. *Anolis desechensis* 2—PUERTO RICO: Isla Desecheo: KdQ 1884. *Anolis distichus*—DOMINICAN REPUBLIC: Distrito Nacional: Parque Infatil: Gregory C. Mayer unnumbered. *Anolis ernestwilliamsi*—BRITISH VIRGIN ISLANDS: Carrot Rock: REG 871. *Anolis evermanni* 1—PUERTO RICO: Humacao: Sierra de Luquillo: 321873. *Anolis evermanni* 2—PUERTO RICO: Humacao: Sierra de Luquillo: 321875. *Anolis gingivinus*—ST. MARTIN: Baie aux Prune: 315553. *Anolis gundlachi* 1—PUERTO RICO: Humacao: Sierra de Luquillo: 321877. *Anolis gundlachi* 2—PUERTO RICO: Humacao: Sierra de Luquillo: 321878. *Anolis krugi* 1—PUERTO RICO: Humacao: Sierra de Luquillo: 321885. *Anolis krugi* 2—PUERTO RICO: Arecibo: Reserva Forestal Cambalache: 321883. *Anolis monensis*—PUERTO RICO: Isla Mona: JBL 885. *Anolis poncensis* 1—PUERTO RICO: Ponce: Punta Cuchara: 321895. *Anolis poncensis* 2—PUERTO RICO: Ponce: Punta Cuchara: 321896. *Anolis pulchellus* 1—PUERTO RICO: Humacao: vicinity of Playa Luquillo: 321900. *Anolis pulchellus* 2—PUERTO RICO: Arecibo: Reserva Forestal Cambalache: 321898. *Anolis scriptus*—BAHAMAS: Inagua: D. Shochat 1861–4. *Anolis stratulus* 1—PUERTO RICO: Arecibo: Reserva Forestal Cambalache: 321904. *Anolis stratulus* 2—PUERTO RICO: Humacao: Sierra de Luquillo: 321906. *Anolis wattsi wattsi*—ANTIGUA: St. Mary's Parish: 321759.